



# An engineered live biotherapeutic for the prevention of antibiotic-induced dysbiosis

Andrés Cubillos-Ruiz<sup>1,2,3</sup>, Miguel A. Alcantar<sup>1,4</sup>, Nina M. Donghia<sup>2</sup>, Pablo Cárdenas<sup>1,4</sup>, Julian Avila-Pacheco<sup>1,3</sup> and James J. Collins<sup>1,2,3,4</sup> ✉

**Antibiotic-induced alterations in the gut microbiota are implicated in many metabolic and inflammatory diseases, increase the risk of secondary infections and contribute to the emergence of antimicrobial resistance. Here we report the design and in vivo performance of an engineered strain of *Lactococcus lactis* that altruistically degrades the widely used broad-spectrum antibiotics  $\beta$ -lactams (which disrupt commensal bacteria in the gut) through the secretion and extracellular assembly of a heterodimeric  $\beta$ -lactamase. The engineered  $\beta$ -lactamase-expression system does not confer  $\beta$ -lactam resistance to the producer cell, and is encoded via a genetically unlinked two-gene biosynthesis strategy that is not susceptible to dissemination by horizontal gene transfer. In a mouse model of parenteral ampicillin treatment, oral supplementation with the engineered live biotherapeutic minimized gut dysbiosis without affecting the ampicillin concentration in serum, precluded the enrichment of antimicrobial resistance genes in the gut microbiome and prevented the loss of colonization resistance against *Clostridioides difficile*. Engineered live biotherapeutics that safely degrade antibiotics in the gut may represent a suitable strategy for the prevention of dysbiosis and its associated pathologies.**

Disruption of the ecological balance in gut microbial communities, termed dysbiosis, has been associated with a wide range of immunological and metabolic disorders such as allergies, autoimmunity and obesity<sup>1</sup>. Antibiotic therapy is essential for treating bacterial infections; however, antibiotic use often induces dysbiosis when systemically circulating antibiotics reach the gut via biliary excretion<sup>2,3</sup>. Since antibiotic presence in the gut is only required when treating gastrointestinal infections, antibiotics should be excluded from the distal gut in all other usage indications to spare the native microbiota. Disturbance of the commensal microbial communities in the gut increases the risk of secondary infections owing to the loss of colonization resistance<sup>1</sup>. Most notably, repeated exposure of the gut microbiota to antibiotics eliminates commensal bacteria from their intestinal niche and opens the opportunity for pathogens such as *Clostridioides difficile* to colonize and proliferate. In their 2019 Antibiotic Resistance Threats Report, the US Centers for Disease Control designated the highest threat level to *C. difficile* infection (CDI), of which ~224,000 yearly cases cause ~13,000 deaths. Exposure to antibiotics also contributes to the emergence of antimicrobial resistance through the enrichment of gut bacterial populations that carry antimicrobial resistance genes (ARGs)<sup>4,5</sup>, which in turn can be transferred to pathogenic bacteria through horizontal gene transfer (HGT)<sup>6,7</sup>. Therefore, there is a pressing need for effective interventions that protect the gut microbiota while antibiotics systemically circulate in the body.

The global yearly usage of antibiotics is ~77 billion doses, of which  $\beta$ -lactams constitute ~48 billion doses (~62%)<sup>8</sup>. The  $\beta$ -lactam antibiotics (penicillins, carbapenems and cephalosporins) are highly effective for treating a variety of bacterial infections; in the United States alone, ~15 million patients receive intravenous  $\beta$ -lactam antibiotics every year<sup>8</sup>. Clinicians often prescribe probiotics during antibiotic treatment as a strategy to repopulate the gut with innocuous bacteria in an attempt to mitigate harmful alterations of the gut

microbiota<sup>9</sup>. However, there are no clearly described mechanisms by which standard probiotic formulations might prevent the loss of native species or replace the multifaceted functions of the endogenous microbiota<sup>10</sup>. Although there are extensive data that support the safety of human supplementation with probiotic microorganisms, the results of studies investigating their clinical efficacy in preventing antibiotic-induced pathologies are often conflicting<sup>10,11</sup>. Moreover, the benefits of post-antibiotic supplementation with probiotics have been challenged by recent studies that suggest their presence might delay the natural recovery of native members of the gut following antibiotic perturbation<sup>12</sup>. Leveraging the utility of food-associated bacteria as safe delivery vectors of biological effectors to the intestine<sup>13</sup>, we created an engineered live biotherapeutic product (eLBP) that, when taken simultaneously with a parenteral  $\beta$ -lactam treatment, could be used as a microbiota-protecting intervention that minimizes dysbiosis and its associated adverse outcomes.

Bacteria have evolved various mechanisms to survive the action of  $\beta$ -lactam antibiotics, including the production of lactam-ring-hydrolysing enzymes, modification of the cell wall target and efflux pumps<sup>14,15</sup>. The most common  $\beta$ -lactam resistance mechanism is the production of  $\beta$ -lactamases, which are enzymes that act near the bacterial cell wall to inactivate  $\beta$ -lactam antibiotics before they bind their target<sup>16</sup>. The expression of these enzymes by pathogenic bacteria greatly increases their fitness under antibiotic selection pressure, and represents a growing threat for the treatment of infections<sup>17</sup>. However, if repurposed through synthetic biology approaches, engineered bacterial expression of  $\beta$ -lactamases may present an effective strategy to eliminate antibiotics from unwanted locations in the body. We hypothesized that transient gut occupancy by an eLBP population secreting a  $\beta$ -lactamase as a 'public good' could prevent the collapse of the gut microbial communities when challenged with a  $\beta$ -lactam antibiotic. Two conditions are needed to

<sup>1</sup>Institute for Medical Engineering and Science, and Synthetic Biology Center, Massachusetts Institute of Technology, Cambridge, MA, USA. <sup>2</sup>Wyss Institute for Biologically Inspired Engineering, Harvard University, Boston, MA, USA. <sup>3</sup>Broad Institute of MIT and Harvard, Cambridge, MA, USA. <sup>4</sup>Department of Biological Engineering, Massachusetts Institute of Technology, Cambridge, MA, USA. ✉e-mail: [jimjc@mit.edu](mailto:jimjc@mit.edu)

make a safe  $\beta$ -lactamase-expressing eLBP. First, the antibiotic degradation trait should not be amenable for HGT to other bacteria. Second, the trait cannot confer a selective advantage to the producing cell over the native microbial communities, to avoid overgrowth of the eLBP in the gut or in the environment. In this Article, we present the generation and evaluation of an engineered *Lactococcus lactis* strain that protects against antibiotic-induced dysbiosis, prevents ARG enrichment and maintains colonization resistance against *C. difficile* in mice receiving parenteral  $\beta$ -lactam treatment.

## Results

**Engineering an extracellular heterodimeric  $\beta$ -lactamase expression system.** We chose to engineer *L. lactis* owing to several features that make it well suited for potential clinical application. *L. lactis* is a Gram-positive bacterium that is usually found in fermented milk products and has been safely consumed in high concentrations for millennia<sup>18</sup>. *L. lactis* is considered a Generally Regarded as Safe (GRAS) organism and has been safely used as a drug delivery vector in multiple human clinical trials<sup>19,20</sup>. In addition, ingested *L. lactis* has been shown to transit through the human gut without long-term colonization and without affecting the composition of the host microbiota<sup>21</sup>. Importantly, *L. lactis* remains metabolically active throughout its gut transit time and represents an ideal system for the transient delivery of biologic effectors to the gut.

We sought to engineer an *L. lactis* strain capable of inactivating  $\beta$ -lactam antibiotics in its environment by secreting a heterodimeric  $\beta$ -lactamase that is encoded in a two-gene biosynthesis strategy (Fig. 1a). By refactoring  $\beta$ -lactam degradation into two genetically unlinked components that independently are non-functional, we remove the selective advantage conferred upon a single locus and limit the possible spread of our engineered trait in the population through a single HGT event. To achieve this, we generated a split version of the TEM-1  $\beta$ -lactamase, termed spTEM1, that regains its activity when reconstituted in the extracellular environment. TEM-1 can be divided into two enzymatically inactive fragments (BLF1 and BLF2) that undergo protein re-folding when brought into close proximity, thus restoring hydrolytic activity<sup>22</sup>. To minimize heterodimer dissociation and enhance the rate at which the active enzyme is reconstituted, we fused the BLF1 and BLF2 fragments to the covalent bond-forming cognate domains SpyTag (ST) and SpyCatcher (SC), respectively<sup>23</sup>. These fusion proteins were cloned into the *L. lactis* spTEM1 strain that constitutively expresses the subunit fragments from independent genetic loci and secretes them via the Usp45 signal peptide for extracellular assembly (Fig. 1a). We used the colorimetric substrate nitrocefin to evaluate the  $\beta$ -lactamase activity in culture supernatants and observed that the ST-BLF1 and SC-BLF2 subunits alone do not display  $\beta$ -lactamase activity; moreover, in the absence of the covalent bond created by the ST and SC interaction, the BLF1 and BLF2 fragments slowly reconstituted showing minimal  $\beta$ -lactamase activity (Fig. 1b). These results demonstrate that the post-translational assembly of heterodimeric fragments derived from the TEM-1  $\beta$ -lactamase restores enzymatic activity and allows the system to be recoded as two independent genetic loci.

**The spTEM1  $\beta$ -lactamase system does not confer ampicillin resistance to producer cells.** Natural  $\beta$ -lactamases confer a strong fitness advantage to producer cells by cleaving  $\beta$ -lactams and preventing cell wall damage. In Gram-negative bacteria,  $\beta$ -lactamases localize to the periplasmic space, which increases their local concentration near the cell wall and enables high levels of resistance to  $\beta$ -lactams<sup>17</sup>. In Gram-positive bacteria,  $\beta$ -lactam resistance generally occurs through alterations to the bacterial cell wall target<sup>14</sup>. However, in several  $\beta$ -lactamase-producing Gram-positive bacterial species, lipoprotein anchors have evolved to keep these enzymes bound to the cell wall and increase their local concentration<sup>14,24</sup>.

Since subcellular localization near the cell wall is a strongly selected trait during the evolution of  $\beta$ -lactamases, we hypothesized that the secretion and extracellular reconstitution features engineered into the *L. lactis* spTEM1 strain would prevent a selective advantage on individual producer cells as the enzyme is free to diffuse away from the cell wall, leaving it unprotected from the antibiotic.

To test this hypothesis, we evaluated the effect of spTEM1 expression and cell density on survival under different concentrations of ampicillin. We found that the expression of the spTEM1  $\beta$ -lactamase system did not confer ampicillin resistance to single cells of *L. lactis* and that survival to the antibiotic is dependent on cell density (Fig. 1c). In contrast, periplasmic localization of the TEM-1  $\beta$ -lactamase in *Escherichia coli* enabled growth in ampicillin as single colonies. To survive the action of ampicillin the *L. lactis* spTEM1 population requires a threshold cell density at which the concentration of extracellular  $\beta$ -lactamase is enough to inactivate the ampicillin in the occupied area. Below this survival density threshold, the entire population collapses before the antibiotic can be inactivated (Fig. 1c). These findings indicate that the expression of the spTEM1  $\beta$ -lactamase system in *L. lactis* does not decrease susceptibility to ampicillin of producer cells, but rather confers the ability to survive ampicillin as an emergent property that depends on population density (Extended Data Fig. 1). Therefore, our engineered extracellular spTEM1  $\beta$ -lactamase serves as a microbial public good that confers no increased advantage to producer cells relative to neighbouring cells. This feature constitutes a biosafety mechanism that is intended to preclude the eLBP from gaining a competitive advantage over native bacteria during ampicillin selection.

**The spTEM1  $\beta$ -lactamase system is not amenable to acquisition by HGT.** The stable acquisition and maintenance of a new genetic trait by HGT requires both the physical mobilization of DNA into the recipient cell and provision of enough selective advantage to ensure fixation in the population. While encoding the spTEM1  $\beta$ -lactamase system in separate genetic loci reduces the likelihood of transfer to a single recipient cell, the scenario of simultaneous acquisition of the two  $\beta$ -lactamase fragments cannot be completely ruled out. Having demonstrated that the spTEM1  $\beta$ -lactamase does not confer resistance to a Gram-positive bacterium such as *L. lactis*, we next investigated whether potential stable acquisition of the spTEM1  $\beta$ -lactamase gene fragments by a Gram-negative bacterium confers a selective advantage in the presence of ampicillin. Since the spTEM1 system is not directly transferable to *E. coli*, we forced stable expression of the spTEM1  $\beta$ -lactamase gene fragments by changing the constructs, so they are harboured in compatible episomes and expressed with compatible promoter sequences. We found that, even in a bacterium with periplasm, the expression of the two spTEM1  $\beta$ -lactamase gene fragments is not sufficient to confer resistance to ampicillin (Fig. 1d). Like *L. lactis* spTEM1, *E. coli* cells expressing the spTEM1  $\beta$ -lactamase system require a threshold cell density to allow for population-level survival as no growth of single colonies was observed. This result, which contrasts with the resistance observed for the native TEM-1  $\beta$ -lactamase, may be due to transport-related incompatibility by the secretion signals used in the spTEM1  $\beta$ -lactamase system that are designed to work specifically with the *L. lactis* machinery. Consequently, even in the scenario where both gene fragments of the spTEM1  $\beta$ -lactamase system are transferred to a Gram-negative cell, the trait cannot provide sufficient protection to endow the recipient with ampicillin resistance, and thus it is unlikely to be acquired by natural selection.

***L. lactis* spTEM1 degrades ampicillin in the intestine without affecting the antibiotic concentration in serum.** We next sought to investigate the effect of intestinal expression of the spTEM1  $\beta$ -lactamase on the pharmacokinetics of ampicillin in a mouse model. We devised a feeding regimen aimed at populating the

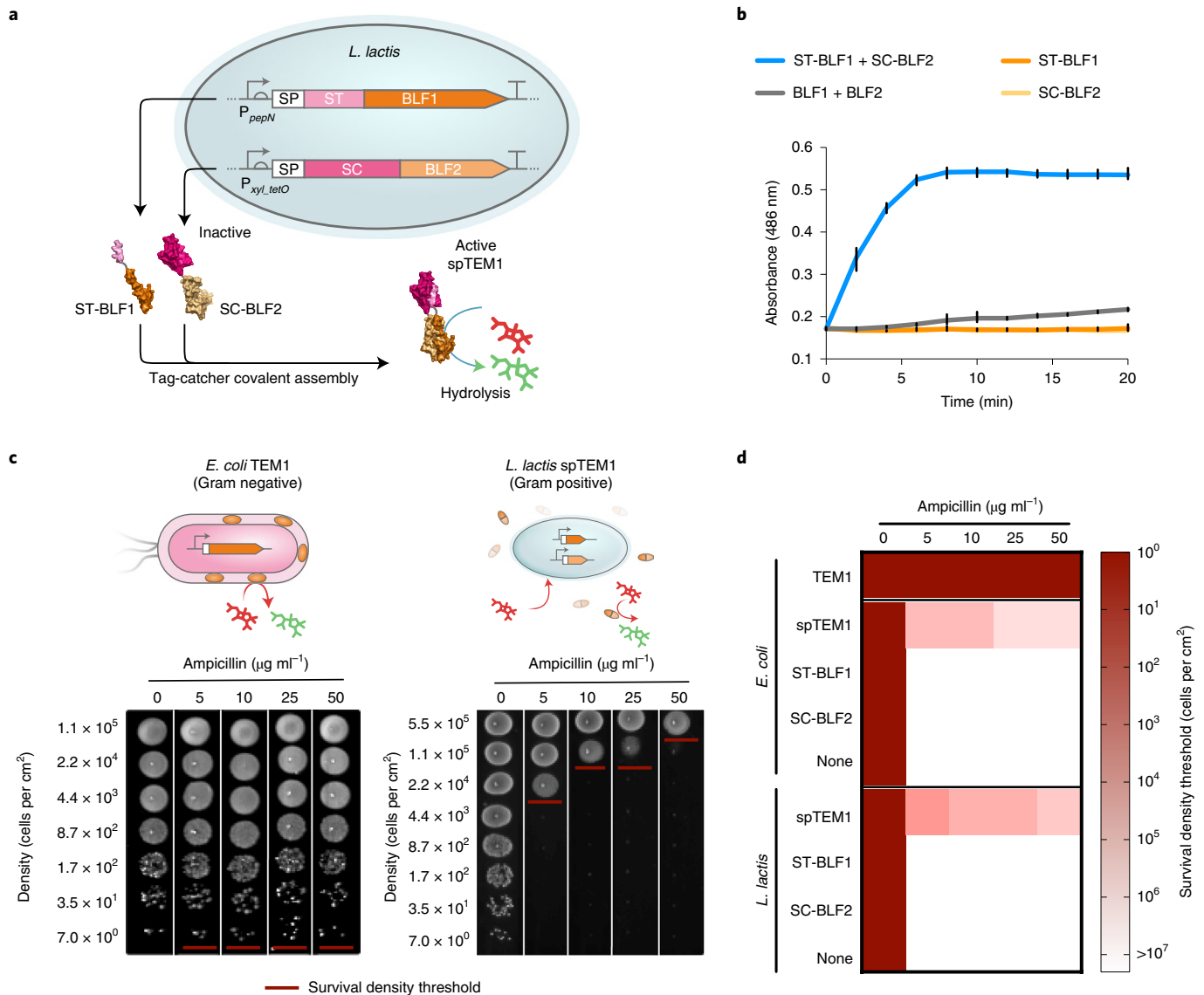


**Fig. 1 | A heterodimeric  $\beta$ -lactamase (spTEM1) system for the extracellular degradation of  $\beta$ -lactam antibiotics. **a**, Schematic representation of the split biosynthesis strategy of the spTEM1  $\beta$ -lactamase in *L. lactis*. The ST-BLF1 and SC-BLF2 subunits are expressed from independent genetic loci and actively secreted for extracellular assembly of the active enzyme. *PepN*, *L. lactis pepN* gene promoter; *PxyL\_tetO*, synthetic promoter derived from the *Bacillus subtilis xyl* promoter; SP, *L. lactis Usp45* signal peptide. **b**, Detection of  $\beta$ -lactamase activity in components of the spTEM1 system using a nitrocefin hydrolysis assay. Covalent bond formation between the ST and SC domains enhances the rate of assembly of the BLF1 and BLF2 subunits and promotes the restoration of enzymatic activity of the spTEM1. Means and standard deviations of  $n = 3$  technical replicates are shown. **c**, Determination of the survival density threshold (red lines) to ampicillin of  $\beta$ -lactamase-expressing bacteria. Native  $\beta$ -lactamases in the periplasm of *E. coli* confer selective advantage to single cells, enabling the formation of single colonies. Ampicillin survival in *L. lactis* spTEM1 is an emergent property of the population and not of single cells; the diffusion of the spTEM1  $\beta$ -lactamase from the *L. lactis* surface precludes protection to the producer cell when the population density is low. **d**, Ampicillin survival density threshold in prototypical Gram-negative and Gram-positive strains expressing elements of the spTEM1 system. Expression of the spTEM1 system in *E. coli* does not confer resistance to single cells. The density values reported in the heat map correspond to the average of three technical replicates.**

mouse gut with the eLBP while ampicillin circulates in the body (Extended Data Fig. 2). To ensure a robust presence of the eLBP in the gut, we orally gavaged  $10^{10}$  colony-forming units (c.f.u.) of *L. lactis* spTEM1 2 h before and then simultaneously with ampicillin administration for a total of two oral eLBP doses per antibiotic injection (Fig. 2a). This eLBP feeding regime achieved an *L. lactis* density in faeces of  $\sim 10^9$  c.f.u. per gram 4 h after the first gavage (Extended Data Fig. 2). Robust in situ expression of the spTEM1  $\beta$ -lactamase was confirmed by incubating faecal samples with the colorimetric substrate nitrocefin (Extended Data Fig. 3). We used mass spectrometry to detect ampicillin and its  $\beta$ -lactamase-derived

degradation products (Supplementary Fig. 1) in the caecum and faeces of mice that were treated with *L. lactis* spTEM1 or with the delivery vehicle (control group). To account for the intrinsic variability between abundance measurements of different animals, we determined the ratio of ampicillin penicilloic acid to ampicillin for each sample. We observed that this ratio was significantly higher in the spTEM1-treated group for faeces collected at 15, 60 and 240 min and for caecal contents collected at 240 min post-ampicillin injection, suggesting that the spTEM1  $\beta$ -lactamase promotes continued degradation of ampicillin in the distal gut of mice, especially at later timepoints (Fig. 2b). Importantly, despite the increased  $\beta$ -lactamase

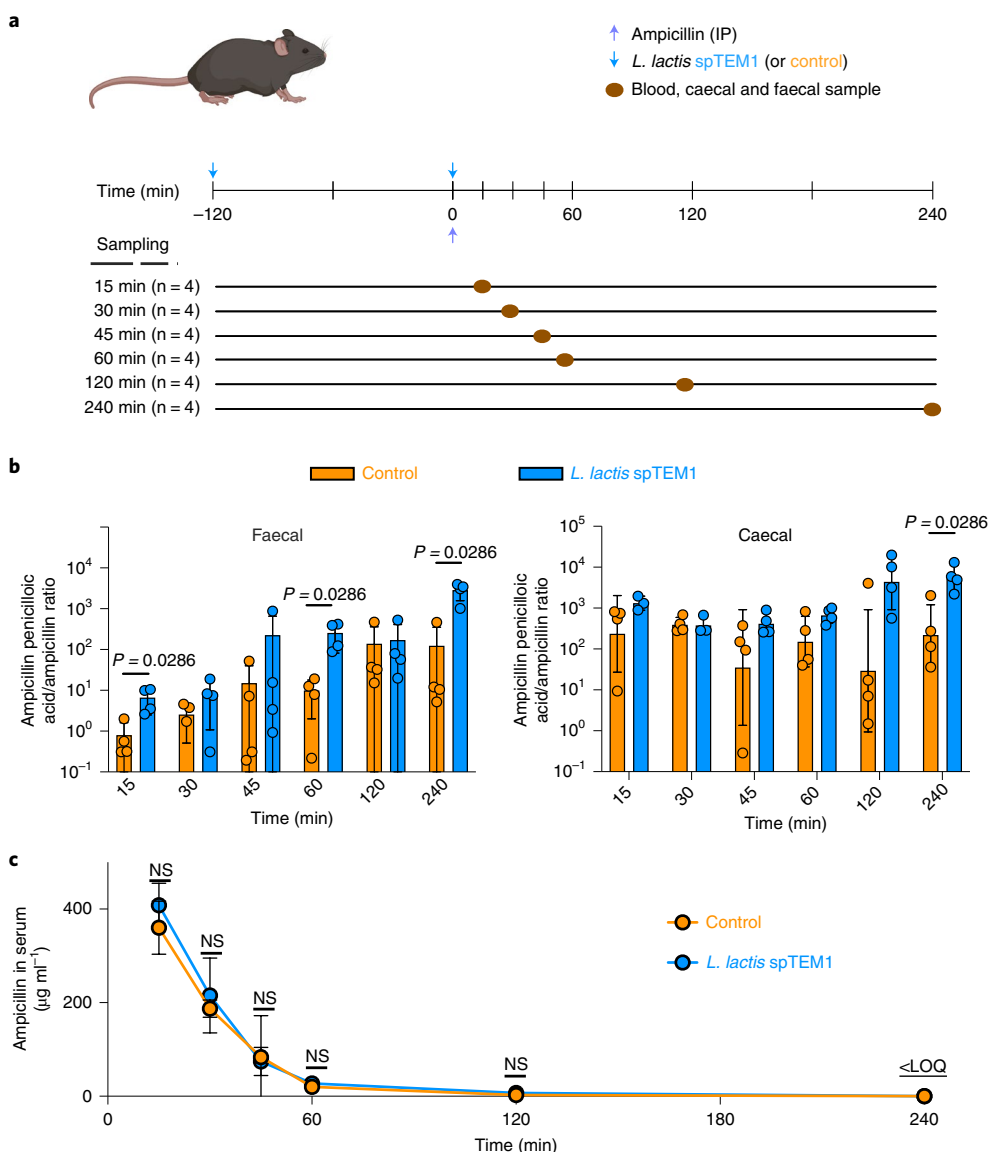


**Fig. 2 | Enzymatic activity of the spTEM1  $\beta$ -lactamase in the mouse intestine does not influence ampicillin concentration in serum.** **a**, Experimental design for testing the effect of *L. lactis* spTEM1 on the pharmacokinetics of ampicillin in mice. **b**, Detection of ampicillin and its degradation products in faeces and caecal contents of mice. Values correspond to the ratio of the abundance of ampicillin penicilloic acid and ampicillin detected by mass spectrometry.  $n = 4$  mice per timepoint. Geometric means and standard deviations of biological replicates are shown. The  $P$  values are shown in the figure and correspond to two-sided Wilcoxon tests between the groups that received *L. lactis* spTEM1 and the control treatment for each timepoint. **c**, Pharmacokinetic curves for ampicillin in serum of mice treated with *L. lactis* spTEM1 or the delivery vehicle control. The ampicillin signal for the 240 min timepoint was below the limit of quantification (LOQ) and was excluded from the curve. Means and standard deviations of biological replicates are shown.  $n = 24$  mice in the *L. lactis* spTEM1 group and  $n = 24$  mice in the control group. Differences in ampicillin serum concentration were not significant (NS) in two-sided Wilcoxon tests between the groups that received *L. lactis* spTEM1 and the control treatment for each timepoint.

activity in the gut, the circulating ampicillin in the serum was not affected at any timepoint, demonstrating that the overall exposure to the antibiotic outside the intestine was maintained (Fig. 2c). This result suggests that the activity of the spTEM1  $\beta$ -lactamase is restricted to the gut and does not affect the bioavailability of ampicillin circulating in the blood, which is critical to ensuring that the antibiotic remains effective for its intended purpose of reaching non-gut sites of infection.

***L. lactis* spTEM1 protects the composition of the gut microbiota after parenteral administration of ampicillin.** To test the efficacy of *L. lactis* spTEM1 in preventing ampicillin-induced dysbiosis, we developed a mouse model that uses susceptibility to CDI as an

endpoint indicator of gut dysbiosis. We determined that a daily intraperitoneal (IP) dose of ampicillin at  $200 \text{ mg kg}^{-1}$  for 3 days was sufficient to abrogate colonization resistance and sensitize the mouse gut to infection with *C. difficile* spores (Extended Data Fig. 4). We used this antibiotic dosing regimen to evaluate whether transient gut colonization by our *L. lactis* spTEM1 strain, which secretes a  $\beta$ -lactamase as a public good, could prevent the collapse of the gut microbial communities after a course of ampicillin (Fig. 3a). We used 16S ribosomal RNA (rRNA) sequencing to characterize the composition of native bacterial communities in ampicillin-treated mice that received either the *L. lactis* spTEM1 strain or the control treatment, which consisted of gavage of the delivery vehicle only. We found that populating the mouse gut with the *L. lactis* spTEM1

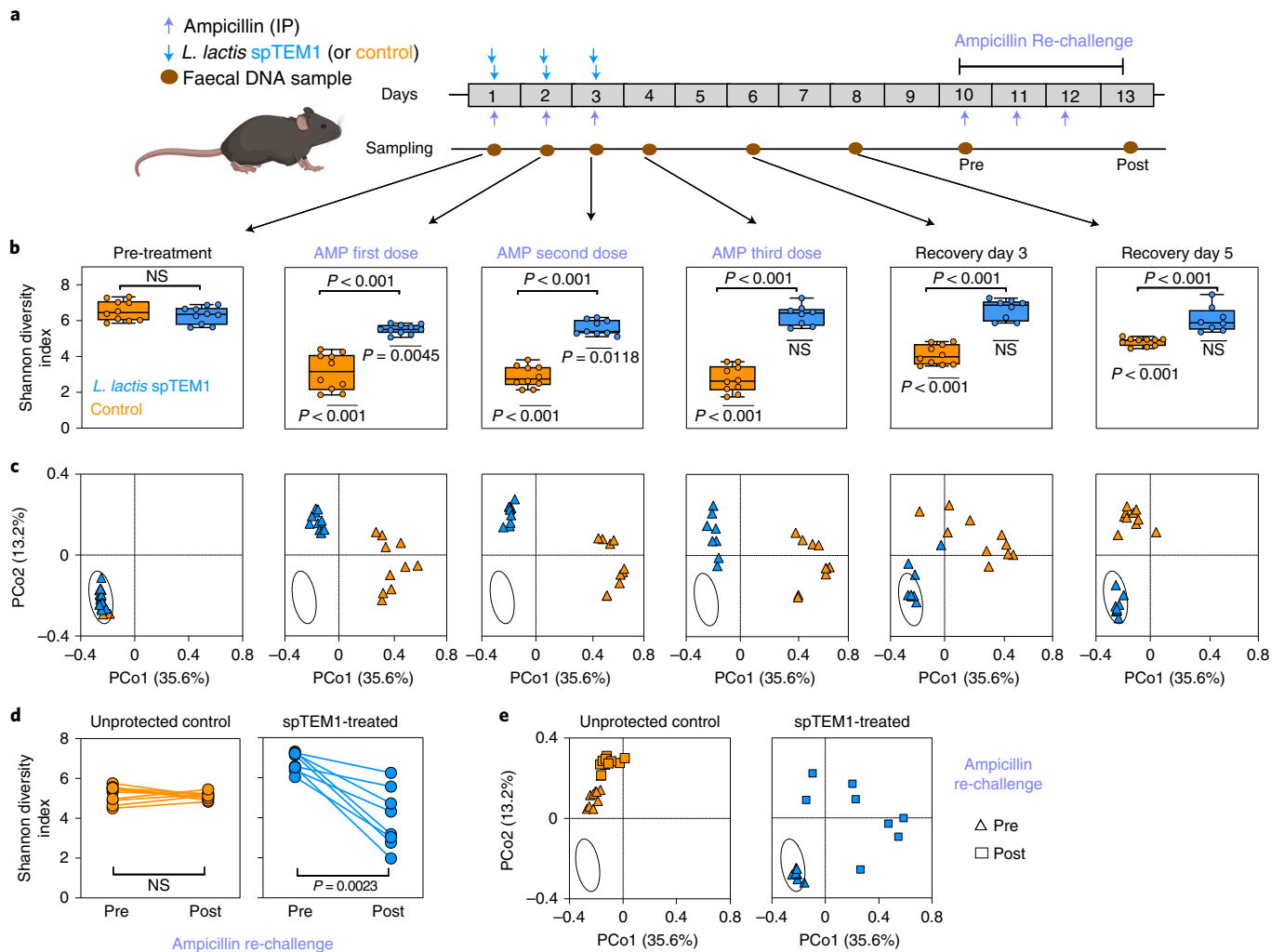


**Fig. 3 | *L. lactis* spTEM1 protects the diversity and composition of the gut microbiota in an ampicillin-induced dysbiosis murine model.** **a**, Experimental design for testing the efficacy of *L. lactis* spTEM1 in preventing dysbiosis by parenteral ampicillin in mice. **b**, Determination of the Shannon diversity index for gut microbial communities in mice before, during and after treatment. The adjusted *P* values correspond to FDR-corrected Wilcoxon tests between the groups that received *L. lactis* spTEM1 and the control treatment. Adjusted *P* values shown below boxes correspond to FDR-corrected two-sided Wilcoxon tests comparing diversity values against baseline diversity at the pre-treatment timepoint. **c**, PCoA of gut microbial communities reveals that treatment with *L. lactis* spTEM1 reduces the impact on  $\beta$ -diversity of ampicillin treatment. Close clustering to pre-ampicillin conditions (denoted as an oval) indicates smaller alteration in the community structure. **d**, Gut microbiota of mice previously treated with *L. lactis* spTEM1 undergo a significant decrease in their diversity after ampicillin re-challenge, indicating that the protective effect of *L. lactis* spTEM1 is transient. Gut microbiota diversity of control-treated mice does not significantly change after ampicillin re-challenge. Adjusted *P* values shown below data points correspond to FDR-corrected two-sided Wilcoxon tests comparing diversity values against baseline diversity at the pre-ampicillin re-challenge timepoint. **e**, PCoA of gut microbiota after ampicillin re-challenge reveals differences in the resulting composition of the community in mice previously treated with *L. lactis* spTEM1 and unprotected mice in the control group, further supporting the transient nature of the eLBP intervention.  $n = 8$  mice in the *L. lactis* spTEM1 group and  $n = 10$  mice in the control group. All box plots display minimum, 25th percentile, median, 75th percentile and maximum of biological replicate measurements. NS, not significant.

strain significantly reduced the impact of ampicillin on the bacterial  $\alpha$ -diversity compared with the intervention with the control treatment. After the 3-day ampicillin treatment, mice in the control group suffered a sharp drop in their bacterial diversity and did not recover to the original values for the remainder of the experiment (Fig. 3b). In contrast, mice that received the *L. lactis* spTEM1 strain maintained a significantly higher Shannon diversity index compared with the control group at all timepoints and fully recovered to their original bacterial baseline diversity values after the third ampicillin dose (Fig. 3b).

We further investigated the effect of the *L. lactis* spTEM1 strain in preventing changes in the taxonomic profile of the gut microbiota upon treatment with ampicillin. Principal coordinate analysis

(PCoA) of the Bray–Curtis dissimilarity of amplicon sequence variants between samples revealed that the composition of gut microbiota of mice receiving *L. lactis* spTEM1 deviated slightly during the 3 days of ampicillin treatment before returning to its original composition. This was evidenced by close clustering with pre-treatment samples in the recovery days after the antibiotic dosing period (Fig. 3c). On the other hand, the gut microbiota of ampicillin-treated mice in the control group suffered profound alterations in their composition that made them diverge from their original state and were not re-clustered even at 7 days after the last ampicillin dose (Fig. 3c). While permutational analysis of variance (PERMANOVA) analysis revealed that the microbial populations were not significantly different only at the pre-treatment timepoint, the  $\beta$ -diversity



*F* statistics with respect to pre-treatment are consistently smaller in the spTEM1 group compared with the control group at all time-points (Supplementary Table 1). We next sought to demonstrate that the protective effect of *L. lactis* spTEM1 is transient and that the antibiotic susceptibility in the gut is restored after the treatment. After 7 days from the last eLBP dose, we subjected the mice in the spTEM1-treated and control groups to a second challenge with ampicillin for 3 days in the absence of any protective intervention (Fig. 3a). We observed that the gut microbiota of mice in the spTEM1-treated group were susceptible again to the action of the antibiotic as evidenced by a decrease in the Shannon diversity index (Fig. 3d) and the disruption of the composition of the  $\beta$ -diversity (Fig. 3e) of each animal post-ampicillin re-challenge. Interestingly, mice in the control-treated group did not suffer significant changes in their diversity after the second ampicillin exposure (Fig. 3d). Since the gut microbiota in the control group did not recover to their original diversity values before the ampicillin re-challenge, it is possible that the lack of sensitivity to the antibiotic is due to the presence of an extant population that is dominated by organisms that were selected for their capacity to withstand the first ampicillin course. These results further demonstrate that antibiotic perturbation causes long-lasting changes in the composition and antibiotic susceptibility profile of gut microbes, underscoring the need for protective interventions during antimicrobial therapy.

***L. lactis* spTEM1 prevents the enrichment of ARGs in mice treated with ampicillin.** Antimicrobial resistance occurs naturally in bacterial communities of diverse environments, including the human gut<sup>25</sup>. The gut microbiome carries an endogenous pool of ARGs that can rapidly expand on exposure to exogenous antimicrobials owing to selection and outgrowth of resistant variants<sup>5,26</sup>. Exposure to one class of antibiotics can also lead to the enrichment of ARGs of unrelated classes of antibiotics and increase the abundance of mobile genetic elements, a phenomenon that is thought to contribute to the emergence of multidrug-resistant pathogens through HGT<sup>1,6</sup>. We investigated whether the community protection provided by expression of spTEM1  $\beta$ -lactamase also alleviates the selective pressure on ARGs after exposure to ampicillin. Specifically, we performed metagenomic shotgun sequencing and mapped the reads to the Comprehensive Antibiotic Resistance Database (CARD)<sup>27</sup> to determine the abundance of ARGs in the mouse faecal samples. We found that ampicillin treatment in mice in the control group resulted in a significant expansion of ARGs (Fig. 4a). The categories of ARGs observed in this increase were related not only to  $\beta$ -lactam antibiotics but also to glycopeptides, non-ribosomal peptides and the macrolide–lincosamide–streptogramin B group, as well as efflux pumps. In contrast, despite ampicillin treatment, the presence of *L. lactis* spTEM1 significantly reduced the expansion and subsequent selection of ARGs from the endogenous pool of the gut microbiome (Fig. 4a). When compared with the pre-treatment baseline, the control group had a significant enrichment of ARGs until the seventh day of recovery (Fig. 4a and Supplementary Table 2). In the spTEM1-treated group, significant ARG enrichment was observed only during the first 2 days of the ampicillin treatment, which demonstrates that the intervention with the eLBP not only reduced the magnitude but also the time that other gut bacteria are exposed to an enriched ARG pool (Fig. 4a and Supplementary Table 2). As expected, upon antibiotic re-challenge, the mice in the spTEM1-treated group showed an increase in the abundance of ARGs, which further demonstrates that the protective effect of *L. lactis* spTEM1 on the gut microbiota is transient (Fig. 4a). Of note, we did not detect a significant increase in the abundance of ARGs in the control group after the second course of ampicillin (Fig. 4a), which suggests that the mechanisms that make an already dysbiotic gut microbiota resilient to a second challenge with ampicillin go beyond the enrichment of ARG in the population.

Our ARG analysis also detected vector-derived sequences from the spTEM1 system, including a chloramphenicol acetyltransferase gene (not shown) that was used to track the eLBP and evaluate the selective pressure on engineered and endogenous  $\beta$ -lactamases during the intervention. Notably, despite having fed the mice with more than  $10^{10}$  c.f.u. *L. lactis* spTEM1 cells during three consecutive days, the spTEM1  $\beta$ -lactamase gene fragments were present only in trace amounts by 3 days after the last eLBP dose and undetectable by 5 days (Fig. 4b). This effective depletion of a large pool of spTEM1 gene fragments contrasts with the strong enrichment and selection of endogenous  $\beta$ -lactamase genes that emerged from a small initial pool in the control group during the first ampicillin course (Fig. 4b). Upon ampicillin re-challenge of the spTEM1-treated group, there was a significant enrichment of endogenous  $\beta$ -lactamase genes, but no spTEM1  $\beta$ -lactamase gene fragments were detected, suggesting that any lingering gene fragments of the spTEM1 system were not under selection despite the ampicillin pressure (Fig. 4b). These results reinforce our claim that the expression of the spTEM1 system does not confer an added selective advantage to producer cells over the gut microbiota in vivo and thus is readily eliminated from the gut microbiome after its intended use. Furthermore, this analysis demonstrates that transient provision of  $\beta$ -lactamase activity in the gut lumen alleviates the selective pressure of ampicillin from the gut microbial population and prevents the enrichment of various classes of ARG.

***L. lactis* spTEM1 maintains colonization resistance against *C. difficile* in ampicillin-treated mice.** To determine the effect of our eLBP intervention in preventing the loss of colonization resistance (Fig. 5a), we challenged mice with  $5 \times 10^3$  spores of *C. difficile* at day 1 post-ampicillin treatment and evaluated the pathogen colonization at 24 h and 48 h post-CDI (Fig. 5b). Since the administration of standard live bacteria may also affect *C. difficile* colonization resistance, we tested our engineered *L. lactis* spTEM1 in comparison with *L. lactis* EV, a strain that carries an empty expression vector. Treatment with *L. lactis* spTEM1 resulted in a significantly higher accumulation of ampicillin penilloic acid in faeces compared with treatment with the control *L. lactis* EV (Fig. 5c), without significantly changing the ampicillin available in serum (Fig. 5d). We found that treatment with the *L. lactis* spTEM1 strain preserved colonization resistance in ampicillin-treated mice (Fig. 5e). Remarkably, except for one mouse that displayed initial low colonization at 24 h post-CDI but that resolved the CDI within the next day, all the mice that received the eLBP strain had undetectable numbers of *C. difficile* in the faeces. In contrast, we observed that all ampicillin-treated mice that received the control strain *L. lactis* EV exhibited high *C. difficile* colonization, to the same extent as observed for eLBP-naive ampicillin-treated mice, indicating that the mere presence of *L. lactis* is not enough to provide colonization resistance. We also determined that the *L. lactis* EV strain does not confer sensitivity to CDI in ampicillin-naive mice, demonstrating that our *L. lactis* chassis does not impact the infection process (Fig. 5e).

We next characterized the composition of native bacterial communities in ampicillin-treated mice that received either the *L. lactis* spTEM1 strain or mice treated with *L. lactis* EV. In agreement with our previous results, we observed that the microbial communities in the spTEM1-treated mice had significantly reduced impact on their  $\alpha$ - and  $\beta$ -diversity (Extended Data Fig. 5 and Supplementary Table 3), as well as on the enrichment of the ARG pool (Extended Data Fig. 6). Contrastingly, treatment with *L. lactis* EV did not protect the microbiota from ampicillin, and the effects on diversity and ARG expansion mirrored the ones observed before for the eLBP control (Extended Data Figs. 5 and 6 and Supplementary Table 3). These results support observations that standard probiotics are not sufficient to shield the gut microbiota from the damaging effects of antibiotics<sup>12</sup>. Additionally, we determined that the 3-day *L. lactis*

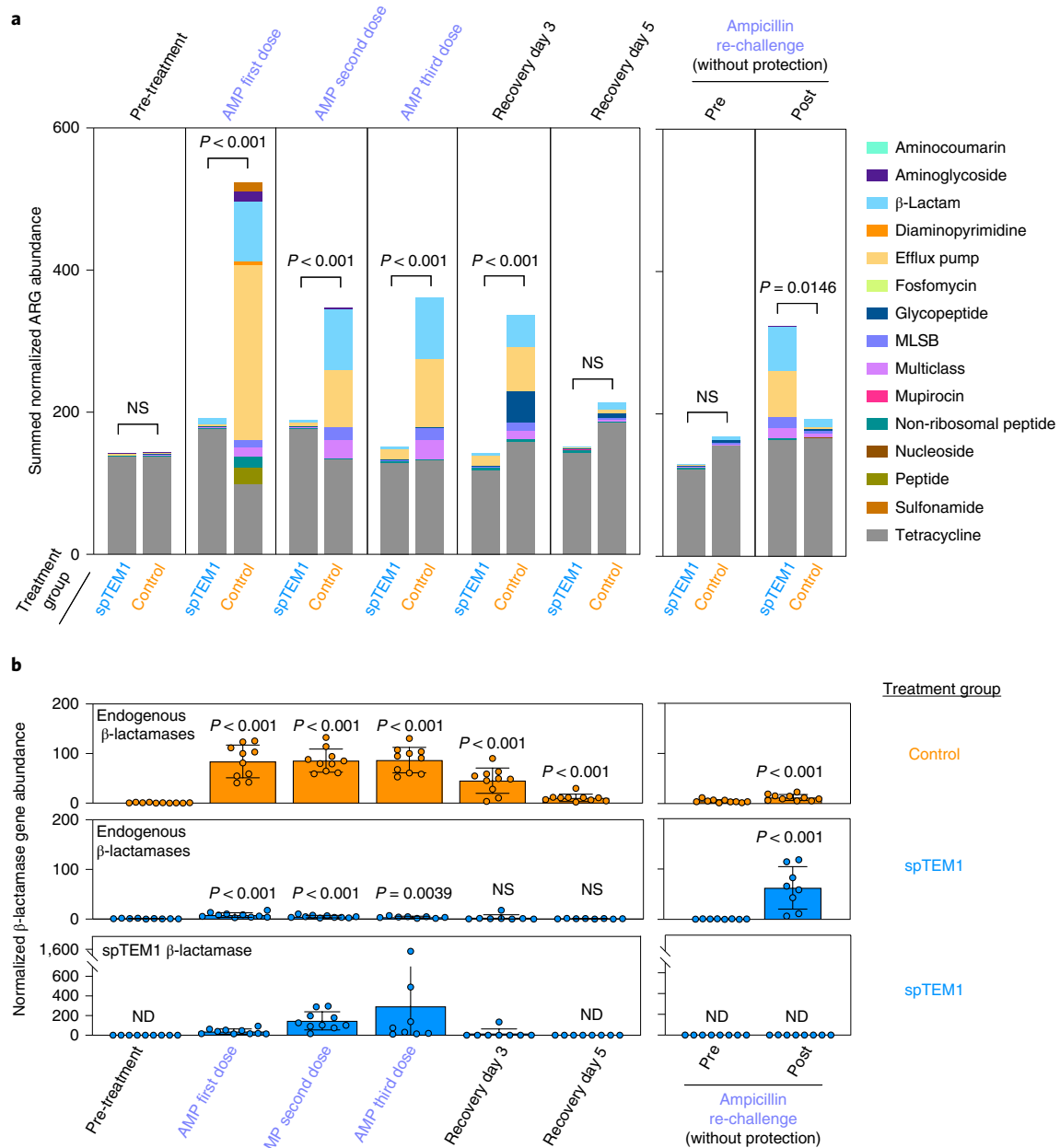


**Fig. 4 | *L. lactis* spTEM1 prevents the enrichment of ARGs following the administration of ampicillin in mice. a**, Analysis of the abundance of ARGs reveals significant enrichment in ampicillin-treated mice receiving the control treatment but not in mice receiving *L. lactis* spTEM1. Stacked bar data are presented as reads mapping the different CARD database categories and normalized to the number of reads in each sample and gene lengths. Adjusted *P* values were calculated with a negative binomial generalized linear model with Tukey's post hoc test between spTEM1-treated and control-treated groups. **b**, Abundance of endogenous and eLBP-derived  $\beta$ -lactamases in mouse faeces. Elimination of the ampicillin selective pressure by the spTEM1  $\beta$ -lactamases reduces the enrichment of endogenous  $\beta$ -lactamases in the mouse gut. Rapid elimination from the system of the spTEM1 gene fragments compared with endogenous  $\beta$ -lactamase genes suggests lack of competitive advantage in the spTEM1 strain.  $n = 8$  mice in the *L. lactis* spTEM1 group and  $n = 10$  mice in the control group. Means and standard deviations of biological replicates are shown. The *P*-value significance corresponds to FDR-corrected two-sided Wilcoxon tests comparing ARG abundance values against baseline values at the pre-treatment timepoint. Means and standard deviations of biological replicates are shown. ND, not detected.

feeding regimen in the absence of ampicillin did not cause a significant change in the Shannon diversity index compared with the pre-treatment condition, which suggests that none of the observed changes in the  $\alpha$ -diversity of the ampicillin-treated mice can be attributed to disturbance of the microbiota by *L. lactis* passage through the gut (Supplementary Fig. 2).

To further define how our eLBP maintains colonization resistance against *C. difficile*, we examined bacterial taxa that were

significantly changed in abundance after the ampicillin treatment compared with their initial state. Consistent with the observed colonization outcomes, the microbiota of mice receiving *L. lactis* EV displayed characteristic abundance changes in bacterial families known to result in loss of resistance to *C. difficile*<sup>28–30</sup>, while the microbiota of mice treated with *L. lactis* spTEM1 did not (Fig. 5f). These changes included a decreased abundance of members of the Lachnospiraceae, Prevotellaceae and Ruminococcaceae groups,

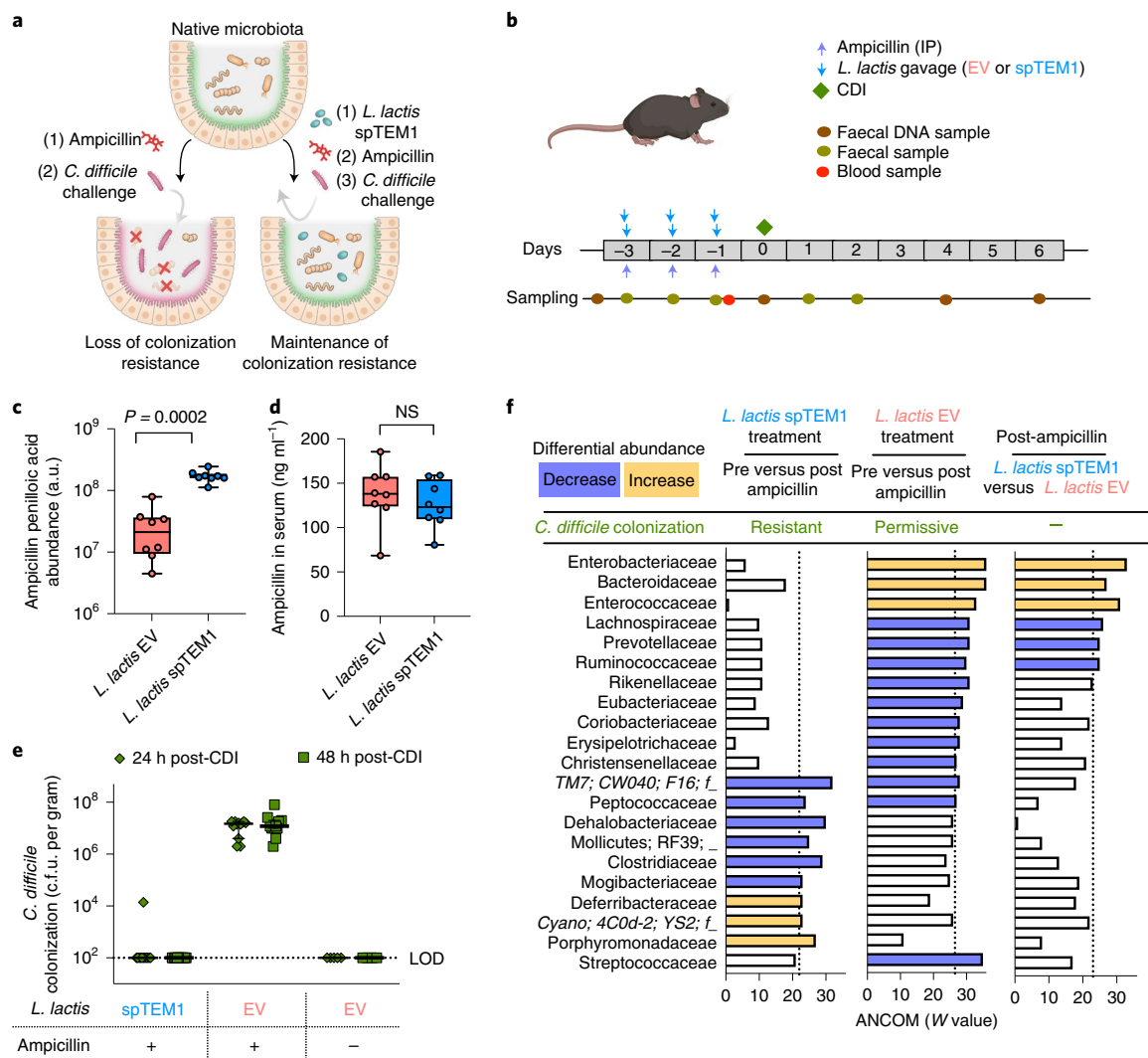


**Fig. 5** | *L. lactis* spTEM1 maintains colonization resistance against *C. difficile* in a mouse model of ampicillin-induced dysbiosis. **a**, Schematic of the eBP strategy for preventing ampicillin-induced loss of colonization resistance against *C. difficile*. **b**, Experimental design for testing the efficacy of *L. lactis* spTEM1 in preventing CDI after parenteral ampicillin in mice. **c**, Increased detection of ampicillin degradation products in mice treated with *L. lactis* spTEM1 ( $n = 8$ ) compared with control treatment ( $n = 8$ ). Values correspond to the abundance values of ampicillin penilloic acid detected by mass spectrometry. The  $P$  value corresponds to unpaired two-sided Wilcoxon tests between groups. **d**, Quantification of ampicillin in serum 30 min after the last IP ampicillin dose reveals no significant differences between mice dosed with *L. lactis* spTEM1 ( $n = 8$ ) and the control *L. lactis* EV ( $n = 8$ ); unpaired two-sided Wilcoxon test,  $P = 0.5054$ . Box plots display minimum, 25th percentile, median, 75th percentile and maximum of biological replicate measurements. **e**, *C. difficile* load in the faeces of ampicillin-treated mouse at 24 h and 48 h post-CDI demonstrates that treatment with *L. lactis* spTEM1 ( $n = 12$  in two independent experiments: first,  $n = 4$ ; second,  $n = 8$ ) prevents loss of colonization resistance while the control strain *L. lactis* EV ( $n = 12$  in two independent experiments: first,  $n = 4$ ; second,  $n = 8$ ) does not. Ampicillin-naïve mice treated with *L. lactis* EV are not susceptible to CDI ( $n = 10$  in two independent experiments: first,  $n = 5$ ; second,  $n = 5$ ). Median and 95% confidence interval for biological replicates are shown. LOD, limit of detection. **f**, ANCOM identifies differential abundance of bacterial populations pre- and post-ampicillin in mice treated with *L. lactis* spTEM1 or *L. lactis* EV. Dashed line indicates the significance cut-off value for the ANCOM  $W$  value. Differential increase or decrease is reported with respect to the first condition stated. 'Resistant' or 'Permissive' indicates the status of the *C. difficile* colonization resistance observed for that group in **e**.

and an increased abundance of the families Enterobacteriaceae, Enterococcaceae and Bacteroidaceae (Fig. 5f). Of note, members of the Lachnospiraceae and Ruminococcaceae families are known to promote a defensive barrier through the production of short-chain fatty acids<sup>31,32</sup> and also encode bile acid  $7\alpha$ -dehydroxylating enzymes that metabolize primary bile acids into secondary bile acids, which are key compounds that inhibit *C. difficile* spores and vegetative cells<sup>33,34</sup>. These alterations in signature bacterial families were also identified when comparing differentially abundant groups between spTEM1-treated and EV-treated mice after ampicillin treatment (Fig. 5f). These data provide strong support to the

notion that *L. lactis* spTEM1 shields the protection-conferring members of the microbiota from the collateral damage of the antibiotic course.

The characterization of the structure of the microbial communities during the proposed dysbiosis-preventing intervention demonstrates that transient colonization of the murine gut by an extracellular  $\beta$ -lactamase-expressing eBP significantly diminishes the loss of bacterial diversity and prevents changes in the composition of the gut microbial communities after the use of parenteral ampicillin. Functionally, the observed level of protection of the native microbiota afforded by *L. lactis* spTEM1 is sufficient to



maintain the microbiota-dependent factors that help exclude *C. difficile* from the gut.

## Discussion

Antibiotic use is the strongest, yet most predictable, disturbance to the gut microbiota. Since the pharmacokinetic properties of clinical-use antibiotics are well characterized, properly timed preventive measures can be designed to minimize the impact of antibiotic presence in the gut. Here we developed an eLBP-based strategy for the prevention of antibiotic-induced gut dysbiosis. Clinical use of a food-associated bacterium that carries an antibiotic degradation trait requires robust safety features, namely the absence of a competitive advantage under antibiotic selection to preclude overgrowth and imperviousness of the trait to HGT. Our eLBP incorporates multiple engineered features that ensure its clinical and environmental safety. First, the secretion and extracellular assembly of the spTEM1  $\beta$ -lactamase preclude self-protection in producer cells and make antibiotic survival a density-dependent property that has effects at the population level, favouring both producer and non-producer cells. Second, while it is impossible to prevent the mobilization of DNA within the microbiome, we refactored  $\beta$ -lactamase function as two separate components to prevent its potential acquisition by natural selection; these individual components do not confer any selective advantage, and they are encoded in independent genetic loci. Third, in the rare event of simultaneous mobilization of the two gene fragments into the same cell, the expression of the spTEM1 is not sufficient to confer resistance, even in *E. coli*, the native host of the TEM-1  $\beta$ -lactamase. Therefore, given the prevailing microbial competition in the gut, the allocation of cellular resources to the production of a suboptimal  $\beta$ -lactamase trait would result in a fitness cost to the recipient cell, which would impair its expansion in the population. Additional safety features could be incorporated into the eLBP, such as chromosomal expression of the spTEM1 system to further reduce the possibility of horizontal mobilization of self-replicating elements and their selectable markers, and the use of previously described auxotrophic *L. lactis* strains to enhance biocontainment outside the gut<sup>35</sup>. Recoding enzymes into physically and functionally separate multi-gene components that are not readily susceptible to natural selection represents a mechanism of biocontainment that safeguards engineered bacterial traits from spreading into wild populations.

Using a mouse model for parenteral ampicillin treatment, we demonstrated that timely oral supplementation with an eLBP that degrades  $\beta$ -lactams prevents the loss of colonization resistance to *C. difficile* by minimizing the loss of diversity and alterations in composition of native commensal bacteria in the gut. While we show that our strategy is effective at protecting microbial groups that determine colonization resistance against *C. difficile*, the same antibiotic-protecting effect may be beneficial for preserving the composition of the microbial groups that are associated with other dysbiosis-related pathologies<sup>36</sup>. Importantly, we showed that the population-level effects of extracellular  $\beta$ -lactamase activity reduce the antibiotic selective pressure on members of the microbiota, which prevents the enrichment of endogenous  $\beta$ -lactamase genes and other determinants of antimicrobial resistance. Since the gut houses the highest density of bacteria in the body, decreasing the size of the pool of ARGs that become available upon  $\beta$ -lactam administration may reduce the rate of acquisition of antimicrobial resistance by pathogenic bacteria or the selection of new  $\beta$ -lactamase variants in the population.

In this study, we used the TEM-1  $\beta$ -lactamase enzyme and ampicillin as a model for  $\beta$ -lactamase/ $\beta$ -lactam pairs of the penicillin class. However, the same design principles of the spTEM1 system can be applied to other  $\beta$ -lactamases with different spectra of  $\beta$ -lactam substrates to extend the reach of the eLBP intervention

to other clinically relevant antibiotics, such as cephalosporins and carbapenems.

The use of preparations of  $\beta$ -lactamase enzymes to degrade  $\beta$ -lactam antibiotics in the gut was described in 2003<sup>37</sup>. Since then, there have been long-standing efforts to develop encapsulated forms of purified  $\beta$ -lactamases for direct intestinal release, for which human clinical trials have recently begun<sup>38,39</sup>. We believe our eLBP strategy will help advance the clinical use of  $\beta$ -lactamases for the protection of the gut microbiota in two aspects. First, the manufacture and scalability of a defined bacterial formulation is significantly easier and less costly than the production and purification of clinical-grade enzymes. Second, our approach is likely to provide a more efficacious release of the active enzyme throughout the intestine, given the continuous metabolic activity of our eLBP. We envision that simple oral administration of our eLBP before parenteral antibiotic administration may significantly reduce the morbidity and mortality associated with antibiotic-related complications of gut dysbiosis.

## Methods

**Bacterial strains.** *Lactococcus lactis* NZ3000 (MoBiTec), a strain for food-grade selection based on its ability to grow on lactose, was used as the parental strain for recombinant gene expression and animal experiments. *L. lactis* was maintained at 30 °C in Difco M17 medium supplemented with 0.5% lactose. *E. coli* NEB 10- $\beta$  (New England BioLabs) cells were used as intermediate hosts for plasmid construction and for assessing survival in cells expressing the spTEM1 system. *E. coli* cells were propagated at 37 °C in LB broth. To enumerate *L. lactis* from mouse faecal samples homogenates, LM17-agar plates supplemented with 2  $\mu$ g ml<sup>-1</sup> rifampicin and 5  $\mu$ g ml<sup>-1</sup> polymyxin B were used as previously reported<sup>40</sup>. *C. difficile* 630 spores were prepared from a single batch and stored long term at 4 °C, as previously reported<sup>41</sup>.

**Construction of *L. lactis* spTEM1.** The class A TEM-1  $\beta$ -lactamase<sup>42</sup> was used as the base for the construction of an engineered heterodimeric  $\beta$ -lactamase named spTEM1. The ST-BLF1 fragment was constructed by fusing the ST sequence<sup>23</sup> to amino acids 26–196 of the TEM-1  $\beta$ -lactamase using a Gly(4)–Ser–Gly(4)–Ser linker. The M182T mutation<sup>42</sup> that increases stability of the enzyme was included in the BLF1 fragment. Similarly, the SC-BLF2 fragment was generated by fusing the SC sequence<sup>23</sup> to amino acids 198–290 of TEM-1  $\beta$ -lactamase using a Gly(4)–Ser–Gly(4)–Ser linker. Both ST-BLF1 and SC-BLF2 contained an N-terminal fusion to the Usp45 signal peptide to achieve extracellular secretion. We used a two-plasmid system to achieve expression of the spTEM1  $\beta$ -lactamase from two independent genetic loci. The ST-BLF-1 fragment was expressed from the plasmid pNZ-ST-BLF-1, which is a derivative of pNZ2122 (MoBiTec, Germany) that uses the *pepN* promoter instead of the *lacA* promoter carried in the base plasmid. The SC-BLF-2 fragment was expressed from the plasmid pLL-SC-BLF-2, which is derived from pECGMC<sup>43</sup>, a shuttle vector with a ColE1 origin of replication for propagation in *E. coli*, an AM $\beta$ 1 origin of replication for *L. lactis* and a chloramphenicol-resistance gene *cat* that can be used for selection in both *E. coli* and *L. lactis*. *L. lactis* EV carries pNZ2122 without any insert and served as the empty vector control.

**$\beta$ -Lactamase assay.** Nitrocefin (BioVision) was dissolved in DMSO to make a 1 mM stock. The stock was added to samples (bacterial culture supernatant or faecal samples in PBS) in a clear-bottom 96-well plate to a final concentration of 0.1 mM. For bacterial culture supernatant, the plate was placed in a spectrophotometer SpectraMaX M5 (Molecular Devices) to read absorbance at 486 nm over time at 37 °C. For the determination of  $\beta$ -lactamase activity in faeces, samples were collected from ampicillin-naive mice 2 h after oral gavage of a single dose of *L. lactis* spTEM1 or after oral gavage of the delivery vehicle. Faecal pellets were incubated statically at room temperature in 250  $\mu$ l of 0.1 mM nitrocefin, and 100  $\mu$ l of supernatant was aspirated for absorbance quantification at 30 and 60 min.

**Determination of the ampicillin survival density threshold.** Bacterial cultures were grown to late exponential phase and collected by centrifugation at 5,000g for 10 min at room temperature. Pellets were washed with fresh medium and collected again. Cell pellets were resuspended in one volume of fresh medium. A series of fivefold dilutions were then prepared to the point of cell density extinction, and 3  $\mu$ l spots of each serial dilution were arrayed onto medium plates containing 0, 5, 10, 25 and 50  $\mu$ g ml<sup>-1</sup> of ampicillin. Plates were incubated for 18 h at the specified temperature for each strain. The expected cell density on each spot was determined on the basis of number of colonies observed in the no-ampicillin control plates and the spot area (~0.79 cm<sup>2</sup>). The survival density threshold was considered the lowest cell density at which bacterial growth is detected as either single colonies or confluent growth. Each measurement was performed three times and the average was reported as the value in the heat map.

**Mouse manipulations.** Six- to 8-week-old female C57BL/6 mice (Charles River Laboratories) were used for the experiments and had a 5-day acclimation period upon arrival to the mouse facility before the beginning of the experiments. Mice were administered ampicillin (Patterson Veterinary) via IP injection. Blood samples were drawn from the submandibular vein at the specified timepoints after ampicillin injection. Two mice out of the initial ten in the spTEM1 group of Fig. 3 died: one because of fluid aspiration after the gavage procedure at day 2 of treatment and the other was accidentally dislocated at day 3 of treatment. All mice in this study were treated in accordance with protocol IS00000852-3, approved by Harvard Medical School Institutional Animal Care and Use Committee and the Committee on Microbiological Safety.

**Preparation of *L. lactis* doses.** *L. lactis* cultures were grown to late exponential phase and collected by centrifugation at 5,000g for 10 min at room temperature. Pellets were washed with fresh medium and collected again. Cell pellets were resuspended in a volume of delivery vehicle that achieved 100-fold concentration. The delivery vehicle used was LM17 medium supplemented with 200 mM phosphate buffer at pH 7.0 to prevent rapid acidification in the concentrated samples. To make 1 M stock of phosphate buffer,  $\text{KH}_2\text{PO}_4$  4.68 g and  $\text{Na}_2\text{HPO}_4$  16.4 g were combined in 100 ml deionized water. The LBP doses were administered in volumes of 150  $\mu\text{l}$  via oral gavage.

**Ampicillin pharmacokinetics assay.** Treatment consisted of oral gavage of  $10^{10}$  c.f.u. of *L. lactis* spTEM1 or the delivery vehicle control 2 h before and simultaneous with a 200 mg  $\text{kg}^{-1}$  IP ampicillin injection. For each timepoint, four animals were euthanized and blood, caecal and faecal samples were collected at 15, 30, 45, 60, 120 and 240 min after the antibiotic injection. Serum, faecal and caecal samples were stored at  $-80^\circ\text{C}$  until analysed by mass spectrometry.

**Mouse gut microbiota protection assays.** Treatment consisted of oral gavage of  $10^{10}$  c.f.u. of *L. lactis* spTEM1 or the delivery vehicle control 2 h before and simultaneous with a 200 mg  $\text{kg}^{-1}$  ampicillin injection for 3 days. Mice were transferred to new cages after the last antibiotic dose. After a 7-day recovery period, mice in the two treatment groups were re-challenged with ampicillin for 3 days. Faecal DNA samples were collected throughout the experiment to monitor microbiota composition.

***C. difficile* infection.** To minimize animal suffering, we chose to use *C. difficile* 630 because it is a low-toxin producer strain with similar colonization capabilities as highly toxigenic strains and produces milder symptoms in mice<sup>44</sup>. A total of  $5 \times 10^3$  spores of *C. difficile* strain 630 were delivered to mice via oral gavage. Antibiotic-treated mice were given 24 h to recover before infection with *C. difficile*. To monitor *C. difficile* colonization, faecal samples were collected, weighed and then moved into an anaerobic chamber to be diluted with anaerobic phosphate-buffered saline. The number of colony-forming units was counted using TCCEFA plates supplemented with 50  $\mu\text{g ml}^{-1}$  erythromycin at  $37^\circ\text{C}$  under anaerobic conditions, as previously reported<sup>45</sup>. eLBP treatment before CDI consisted of  $10^{10}$  c.f.u. of *L. lactis* spTEM1 or the control strain *L. lactis* EV 2 h before and simultaneous with the 200 mg  $\text{kg}^{-1}$  ampicillin injection for 3 days. CDI was performed with  $5 \times 10^3$  spores at 24 h post-treatment. Faecal samples were collected throughout the experiment to monitor pathogen colonization and microbiota composition. A blood sample was collected 30 min after the last ampicillin dose to measure its concentration in serum.

**Detection of ampicillin compounds by mass spectrometry.** Ampicillin estimates in bacterial culture supernatants, serum, caecum and faeces were obtained using a previously described hydrophilic liquid chromatography mass spectrometry method<sup>46</sup>. Faecal and caecal samples were homogenized in ten volumes of water for 4 min at 25 Hz in a Tissue Lyser II (Qiagen). Polar metabolites from samples and aqueous caecal and faecal homogenates (10  $\mu\text{l}$ ) were extracted via protein precipitation with 74.9:24.9:0.2 (v/v/v) acetonitrile/methanol/formic acid containing stable isotope-labelled internal standards (valine-d8, Sigma-Aldrich; and phenylalanine-d8, Cambridge Isotope Laboratories). Cleared extracts were injected onto a 150  $\times$  2 mm Atlantis HILIC column (Waters) using a Nexera X2 U-HPLC system (Shimadzu Scientific Instruments). The abundance of eluting metabolites was estimated using an HF hybrid quadrupole orbitrap mass spectrometer (Thermo Fisher Scientific). The retention time and ampicillin concentration in serum were estimated using a calibration curve made with pooled mouse serum spiked with increasing concentrations of Ampicillin-d5 (A634302 Toronto Research Chemicals). The peaks corresponding to ampicillin, ampicillin-d5 and ampicillin degradation products were manually extracted from the raw data using TraceFinder software (version 3.3, Thermo Fisher Scientific). One caecal sample (1C25) at the 15 min timepoint and another caecal sample (1C29) at the 30 min timepoint in the spTEM1-treated group failed to produce usable MS signal and were discarded from the analysis. Tandem mass spectrometry was conducted using an Orbitrap ID-X Tribrid Mass Spectrometer (Thermo Fisher Scientific).

**DNA extraction and sequencing protocols.** Total genomic DNA was extracted from mouse faecal samples using the QIAamp PowerFecal Pro DNA Kit according to the manufacturer's instructions. Extracted DNA of samples was sent to the MIT

BioMicroCenter for multiplexed amplicon library preparation, covering the 16S rRNA gene V4 region using a dual-index barcode protocol, followed by Illumina MiSeq 16S rRNA gene sequencing.

**16S rDNA data processing.** 16S data were received as de-multiplexed sequences and processed using QIIME 2 (Core 2020.2 distribution)<sup>46</sup>. The same procedures were carried out for the spTEM1 versus control (dataset 1) and spTEM1 versus EV (dataset 2) sequences, unless otherwise noted. First, de-multiplexed sequences were stored in a QIIME 2 artefact using the qiime tools import command with parameters type 'SampleData(PairedEndSequencesWithQuality)'-input-format PairedEndFastqManifestPhred33V2. To remove diversity regions and primers from subsequent analyses, we trimmed the first 23 bp and 20 bp from forward and reverse reads, respectively. Additionally, reads were truncated when the median read quality, from a random subset of 10,000 reads, consistently fell below 30. This quality threshold corresponded to truncating forward reads at 200 bp and reverse reads at 170 bp for dataset 1. Similarly, for dataset 2, forward reads were truncated at 275 bp and reverse reads at 220 bp. Processed sequences (that is, quality trimmed and filtered) were used to create a feature table containing amplicon sequence variants, equivalent to operational taxonomic units clustered at 100% similarity. The aforementioned denoising and feature table construction, in addition to dereplication and chimera removal, were carried out using the QIIME 2 DADA2 plugin<sup>47</sup>. The DADA2 plugin pipeline was implemented with the qiime dada2 denoise-paired command with parameters p-trim-left-f 23-p-trim-left-r 20-p-trunc-len-f 200-p-trunc-len-r 170 (for dataset 1) or p-trim-left-f 23-p-trim-left-r 20-p-trunc-len-f 275-p-trunc-len-r 220 (for dataset 2).

**Taxonomic classification.** To assign taxonomies to the processed sequences, we used a naive Bayes classifier trained on the Greengenes v13.8 99% operational taxonomic unit dataset<sup>48,49</sup>. From the Greengenes dataset, we extracted reference reads corresponding to the 16S region amplified in our dataset using the qiime feature-classifier extract reads command with parameters p-f-primer GTGCCAGCMGCCGCGGTAA-p-r-primer GGACTACHVGGGTWTCTAA T-p-min-length 100-p-max-length 400. This reference read extraction procedure helps increase the prediction accuracy of the naive Bayes classifier by ensuring that the reference reads used for training closely match the 16S region amplified and processed in our dataset. Taxonomic predictions were then carried out with the qiime feature-classifier classify-sklearn command<sup>50</sup> with default parameters.

**Microbial diversity analysis.** Alpha- and  $\beta$ -diversity analyses were carried out using the QIIME 2 diversity plugin. First, a phylogenetic tree was created by: (1) performing a multiple sequence alignment of representative sequences using MAFFT<sup>51,52</sup>, and (2) filtering the alignment to remove highly variable positions, which subsequently enabled the construction of an unrooted and rooted tree using the FastTree programme<sup>53,54</sup>. This tree-creation pipeline was implemented with the qiime phylogeny align-to-tree-mafft-fasttree command with default parameters. Alpha- and  $\beta$ -diversity metrics were then calculated using the qiime diversity core-metrics-phylogenetic command with p-sampling-depth 15054 (for dataset 1) or p-sampling-depth 59900 (for dataset 2). These sampling depths were chosen as they were the largest depths possible without excluding more than one sample; only sample 9T2, from dataset 1, failed to meet this criterion and was excluded from diversity analyses. Statistical comparisons for  $\alpha$ -diversity values were carried out in R v3.6.1 using the pairwise.wilcox.test function with p.adjust.method = 'fdr' (Benjamini-Hochberg)<sup>55</sup> and exact = FALSE. Only the Wilcoxon rank-sum test was performed because of sample drop-out that prevented the use of paired statistical tests. For  $\beta$ -diversity values, PERMANOVA with 999 permutations and false discovery rate (FDR) correction was carried out using the qiime diversity beta-group-significance command with parameter p-pairwise. Alpha-diversity values produced by the qiime diversity core-metrics-phylogenetic command and  $\beta$ -diversity principal coordinate values were exported and plotted using PRISM v8.4.1 (GraphPad).

**Differential abundance analysis.** Differential abundance was calculated using analysis of composition of microbiomes (ANCOM)<sup>56</sup>, which was implemented with the QIIME 2 composition plugin. For pairwise comparisons, the feature table was filtered to obtain the treatment groups and/or timepoints of interest. All comparisons were carried out at the family level (that is, level 5 of Greengenes taxonomy). To conduct comparisons at the family level, feature tables were collapsed at the family level using the qiime taxa collapse command with parameter p-level 5. Pseudocounts were added to this collapsed table using the qiime composition add-pseudocount command with default parameters. Lastly, ANCOM was carried out using the qiime composition ancom command with default parameters.

**Metagenomic analysis.** Reads were first trimmed and filtered using Cutadapt<sup>57</sup> v1.18 and Sickle<sup>58</sup> v1.33 with parameters pe -q 20 -l 30. Host DNA was removed using paired-end mapping with Bowtie2<sup>59</sup> v2.2.6 against mouse reference genome GCF\_000001635.26\_GRCm38.p6. In brief, a bowtie sequence index database was created from the mouse reference genome using bowtie2-build with default parameters and paired-end sequences were mapped to this database using bowtie2

-x with default parameters. Unmapped reads, in which both reads were unmapped to the mouse reference genome, were extracted using SAMtools<sup>60</sup> v1.6 with parameters `view -b -f 12 -F 256`.

To obtain ARG abundances, filtered reads were mapped to the CARD<sup>27</sup> protein homologue model version v3.0.9, as previously described<sup>61</sup>. The CARD protein homologue model contains over 2,000 curated sequences of bacterial genes conferring antibiotic resistance. To this CARD protein homologue model sequence database, we manually included three additional coding sequences corresponding to eLBP-derived genes coding for chloramphenicol resistance and each half of the split  $\beta$ -lactamase enzyme. Including these three eLBP-derived coding sequences helped distinguish ARG reads originating from our eLBP and commensal gut microbiota; the combination of the CARD protein homologue model and the three appended eLBP-derived coding sequences is hereafter referred to as the 'custom CARD database'. To map reads onto this database, a bowtie sequence index database was created from sequences contained in the custom CARD database using bowtie2-build with default parameters. Paired end sequences were mapped to the custom CARD database with Bowtie2 using parameters `-D 20 -R 3 -N 1 -L 20 -i S,1,0,50`, and SAMtools was then used to filter and count the number of reads that mapped to sequences in the custom CARD database. In cases where both forward and reverse reads mapped to the same gene, the reads were counted as one hit. In cases where both reads mapped to different genes, the reads were each counted as one hit to each respective gene. For each sample, mapped read counts (C) for each gene were normalized by gene length (L) and total number of filtered forward and reverse reads (R) using  $C_{\text{norm}} = \frac{C}{\left(\frac{L}{10^3}\right)\left(\frac{R}{10^6}\right)}$  where  $C_{\text{norm}}$  represents normalized gene count. Gene length and number of reads were divided by  $10^3$  and  $10^6$ , respectively, to represent gene length in kilobases and number of reads in millions.

Genes with normalized counts  $>0$  in any sample were kept for further analyses. One sample from the pre-ampicillin timepoint in the *L. lactis* spTEM1 group (4T0) was removed from dataset 1 and one sample from post-ampicillin/pre-CDI timepoint in the *L. lactis* spTEM1 group (T4-9) was removed from dataset 2, as they both failed to produce any reads in the sequencing run. Using annotations available in CARD, genes were manually grouped into 17 major resistance classes: aminocoumarin, aminoglycoside,  $\beta$ -lactam, chloramphenicol, diaminopyrimidine, efflux pump (including putative tetracycline efflux pumps), fosfomicin, glycopeptide, MLSB (macrolide, lincosamide or streptogramin B), multiclass (that is, resistance to multiple antibiotic classes; excludes efflux pumps), mupirocin, non-ribosomal peptide, nucleoside, peptide, rifamycin, sulfonamide and tetracycline. For each treatment group and timepoint, stacked bar plots were created by summing normalized gene counts for each major resistance class within and across samples, and then dividing by the number of samples in each respective treatment group. Statistical analysis was done in R v3.6.1 and plots were generated using GraphPad Prism 8 (GraphPad). Statistical significance of differences in normalized abundance for each resistance class was assessed using negative binomial generalized linear models in the MASS package<sup>62</sup> v7.3-54 with Tukey's post hoc test<sup>63</sup>. ARG annotation tables were organized into data objects using phyloseq<sup>64</sup>.

**Reporting Summary.** Further information on research design is available in the Nature Research Reporting Summary linked to this article.

## Data availability

The main data supporting the results in this study are available within the paper and its Supplementary Information. All DNA sequence data generated in this study are available from the Sequence Read Archive with accession number PRJNA803721. Source data are provided with this paper.

## Code availability

All code for the 16S rDNA analysis and for the metagenomics analysis are available on GitHub at <https://github.com/maalcantar/eLBP-prevents-dysbiosis-16s-analysis> and <https://github.com/maalcantar/eLBP-prevents-dysbiosis-metagenomics-analysis>.

Received: 16 December 2020; Accepted: 18 February 2022;  
Published online: 11 April 2022

## References

- Becattini, S., Taur, Y. & Pamer, E. G. Antibiotic-induced changes in the intestinal microbiota and disease. *Trends Mol. Med.* **22**, 458–478 (2016).
- Karachalios, G. & Charalabopoulos, K. Biliary excretion of antimicrobial drugs. *Chemotherapy* **48**, 280–297 (2002).
- Ghibellini, G., Leslie, E. M. & Brouwer, K. L. Methods to evaluate biliary excretion of drugs in humans: an updated review. *Mol. Pharm.* **3**, 198–211 (2006).
- Stecher, B., Maier, L. & Hardt, W. D. 'Blooming' in the gut: how dysbiosis might contribute to pathogen evolution. *Nat. Rev. Microbiol.* **11**, 277–284 (2013).
- Modi, S. R., Lee, H. H., Spina, C. S. & Collins, J. J. Antibiotic treatment expands the resistance reservoir and ecological network of the phage metagenome. *Nature* **499**, 219–222 (2013).
- Kent, A. G., Vill, A. C., Shi, Q., Satlin, M. J. & Brito, I. L. Widespread transfer of mobile antibiotic resistance genes within individual gut microbiomes revealed through bacterial Hi-C. *Nat. Commun.* **11**, 4379 (2020).
- Modi, S. R., Collins, J. J. & Relman, D. A. Antibiotics and the gut microbiota. *J. Clin. Invest.* **124**, 4212–4218 (2014).
- WHO Report on Surveillance of Antibiotic Consumption: 2016–2018 Early Implementation (World Health Organization, 2018).
- Draper, K., Ley, C. & Parsonnet, J. Probiotic guidelines and physician practice: a cross-sectional survey and overview of the literature. *Benef. Microbes* **8**, 507–519 (2017).
- Suez, J., Zmora, N., Segal, E. & Elinav, E. The pros, cons, and many unknowns of probiotics. *Nat. Med.* **25**, 716–729 (2019).
- Hempel, S. et al. Safety of probiotics to reduce risk and prevent or treat disease. *Evid. Rep. Technol. Assess.* **200**, 1–645 (2011).
- Suez, J. et al. Post-antibiotic gut mucosal microbiome reconstitution is impaired by probiotics and improved by autologous FMT. *Cell* **174**, 1406–1423.e16 (2018).
- Bermudez-Humaran, L. G. et al. Engineering lactococci and lactobacilli for human health. *Curr. Opin. Microbiol.* **16**, 278–283 (2013).
- Fisher, J. F. & Mobashery, S.  $\beta$ -Lactam resistance mechanisms: Gram-positive bacteria and *Mycobacterium tuberculosis*. *Cold Spring Harb. Perspect. Med.* **6**, a025221 (2016).
- Wright, G. D. Bacterial resistance to antibiotics: enzymatic degradation and modification. *Adv. Drug Deliv. Rev.* **57**, 1451–1470 (2005).
- Bush, K. Past and present perspectives on  $\beta$ -lactamases. *Antimicrob. Agents Chemother.* **62**, e01076–18 (2018).
- Bush, K. & Bradford, P. A. Epidemiology of  $\beta$ -lactamase-producing pathogens. *Clin. Microbiol. Rev.* **33**, e00047–19 (2020).
- Teuber, M. in *The Genera of Lactic Acid Bacteria* (eds Wood, B. J. B. & Holzapfel, W. H.) 173–234 (Springer, 1995).
- Limaye, S. A. et al. Phase 1b, multicenter, single blinded, placebo-controlled, sequential dose escalation study to assess the safety and tolerability of topically applied AG013 in subjects with locally advanced head and neck cancer receiving induction chemotherapy. *Cancer* **119**, 4268–4276 (2013).
- Braat, H. et al. A phase I trial with transgenic bacteria expressing interleukin-10 in Crohn's disease. *Clin. Gastroenterol. Hepatol.* **4**, 754–759 (2006).
- Zhang, C. et al. Ecological robustness of the gut microbiota in response to ingestion of transient food-borne microbes. *ISME J.* **10**, 2235–2245 (2016).
- Galarneau, A., Primeau, M., Trudeau, L.-E. & Michnick, S. W.  $\beta$ -Lactamase protein fragment complementation assays as in vivo and in vitro sensors of protein-protein interactions. *Nat. Biotechnol.* **20**, 619–622 (2002).
- Zakeri, B. et al. Peptide tag forming a rapid covalent bond to a protein, through engineering a bacterial adhesin. *Proc. Natl Acad. Sci. USA* **109**, E690–E697 (2012).
- Nielsen, J. B. & Lampen, J. O. Membrane-bound penicillinases in Gram-positive bacteria. *J. Biol. Chem.* **257**, 4490–4495 (1982).
- Forsberg, K. J. et al. The shared antibiotic resistome of soil bacteria and human pathogens. *Science* **337**, 1107–1111 (2012).
- Jernberg, C., Lofmark, S., Edlund, C. & Jansson, J. K. Long-term ecological impacts of antibiotic administration on the human intestinal microbiota. *ISME J.* **1**, 56–66 (2007).
- Alcock, B. P. et al. CARD 2020: antibiotic resistome surveillance with the comprehensive antibiotic resistance database. *Nucleic Acids Res.* **48**, D517–D525 (2020).
- Buffie, C. G. et al. Precision microbiome reconstitution restores bile acid mediated resistance to *Clostridium difficile*. *Nature* **517**, 205–208 (2015).
- Schubert, A. M., Sinani, H. & Schloss, P. D. Antibiotic-induced alterations of the murine gut microbiota and subsequent effects on colonization resistance against *Clostridium difficile*. *mBio* **6**, e00974 (2015).
- Crobach, M. J. T. et al. Understanding *Clostridium difficile* colonization. *Clin. Microbiol. Rev.* **31**, e00021–17 (2018).
- Theriot, C. M. et al. Antibiotic-induced shifts in the mouse gut microbiome and metabolome increase susceptibility to *Clostridium difficile* infection. *Nat. Commun.* **5**, 3114 (2014).
- Wong, J. M. W., de Souza, R., Kendall, C. W. C., Emam, A. & Jenkins, D. J. A. Colonic health: fermentation and short chain fatty acids. *J. Clin. Gastroenterol.* **40**, 235–243 (2006).
- Theriot, C. M., Bowman, A. A. & Young, V. B. Antibiotic-induced alterations of the gut microbiota alter secondary bile acid production and allow for *Clostridium difficile* spore germination and outgrowth in the large intestine. *mSphere* **1**, e00045–15 (2016).
- Lewis, B. B., Carter, R. A. & Pamer, E. G. Bile acid sensitivity and in vivo virulence of clinical *Clostridium difficile* isolates. *Anaerobe* **41**, 32–36 (2016).
- Steidler, L. et al. Biological containment of genetically modified *Lactococcus lactis* for intestinal delivery of human interleukin 10. *Nat. Biotechnol.* **21**, 785–789 (2003).



36. Schwartz, D. J., Langdon, A. E. & Dantas, G. Understanding the impact of antibiotic perturbation on the human microbiome. *Genome Med.* **12**, 82 (2020).
37. Harmoinen, J. et al. Enzymic degradation of a  $\beta$ -lactam antibiotic, ampicillin, in the gut: a novel treatment modality. *J. Antimicrob. Chemother.* **51**, 361–365 (2003).
38. Kaleko, M. et al. Development of SYN-004, an oral  $\beta$ -lactamase treatment to protect the gut microbiome from antibiotic-mediated damage and prevent *Clostridium difficile* infection. *Anaerobe* **41**, 58–67 (2016).
39. Kokai-Kun, J. F. et al. Use of ribaxamase (SYN-004), a  $\beta$ -lactamase, to prevent *Clostridium difficile* infection in  $\beta$ -lactam-treated patients: a double-blind, phase 2b, randomised placebo-controlled trial. *Lancet Infect. Dis.* **19**, 487–496 (2019).
40. Mao, N., Cubillos-Ruiz, A., Cameron, D. E. & Collins, J. J. Probiotic strains detect and suppress cholera in mice. *Sci. Transl. Med.* **10**, eaao2586 (2018).
41. Edwards, A. N. & McBride, S. M. Isolating and purifying *Clostridium difficile* spores. *Methods Mol. Biol.* **1476**, 117–128 (2016).
42. Salverda, M. L., De Visser, J. A. & Barlow, M. Natural evolution of TEM-1  $\beta$ -lactamase: experimental reconstruction and clinical relevance. *FEMS Microbiol. Rev.* **34**, 1015–1036 (2010).
43. Cameron, D. E. & Collins, J. J. Tunable protein degradation in bacteria. *Nat. Biotechnol.* **32**, 1276–1281 (2014).
44. Theriot, C. M. et al. Cefoperazone-treated mice as an experimental platform to assess differential virulence of *Clostridium difficile* strains. *Gut Microbes* **2**, 326–334 (2011).
45. Winston, J. A., Thanissery, R., Montgomery, S. A. & Theriot, C. M. Cefoperazone-treated mouse model of clinically-relevant *Clostridium difficile* strain R20291. *J. Vis. Exp.* **10**, 54850 (2016).
46. Bolyen, E. et al. Reproducible, interactive, scalable and extensible microbiome data science using QIIME 2. *Nat. Biotechnol.* **37**, 852–857 (2019).
47. Callahan, B. J. et al. DADA2: high-resolution sample inference from Illumina amplicon data. *Nat. Methods* **13**, 581–583 (2016).
48. DeSantis, T. Z. et al. Greengenes, a chimera-checked 16S rRNA gene database and workbench compatible with ARB. *Appl. Environ. Microbiol.* **72**, 5069–5072 (2006).
49. McDonald, D. et al. An improved Greengenes taxonomy with explicit ranks for ecological and evolutionary analyses of bacteria and archaea. *ISME J.* **6**, 610–618 (2012).
50. Bokulich, N. A. et al. Optimizing taxonomic classification of marker-gene amplicon sequences with QIIME 2's q2-feature-classifier plugin. *Microbiome* **6**, 90 (2018).
51. Kuraku, S., Zmasek, C. M., Nishimura, O. & Katoh, K. aLeaves facilitates on-demand exploration of metazoan gene family trees on MAFFT sequence alignment server with enhanced interactivity. *Nucleic Acids Res.* **41**, W22–W28 (2013).
52. Katoh, K., Rozewicki, J. & Yamada, K. D. MAFFT online service: multiple sequence alignment, interactive sequence choice and visualization. *Brief. Bioinform.* **20**, 1160–1166 (2019).
53. Price, M. N., Dehal, P. S. & Arkin, A. P. FastTree: computing large minimum evolution trees with profiles instead of a distance matrix. *Mol. Biol. Evol.* **26**, 1641–1650 (2009).
54. Price, M. N., Dehal, P. S. & Arkin, A. P. FastTree 2—approximately maximum-likelihood trees for large alignments. *PLoS ONE* **5**, e9490 (2010).
55. Benjamini, Y. & Hochberg, Y. Controlling the false discovery rate: a practical and powerful approach to multiple testing. *J. R. Stat. Soc. Ser. B* **57**, 289–300 (1995).
56. Mandal, S. et al. Analysis of composition of microbiomes: a novel method for studying microbial composition. *Microb. Ecol. Health Dis.* **26**, 27663 (2015).
57. Martin, M. Cutadapt removes adapter sequences from high-throughput sequencing reads. *EMBnet J.* **17**, 10–12 (2011).
58. Joshi, N. A. & Fass, J. N. Sickle: A sliding-window, adaptive, quality-based trimming tool for FastQ files. <https://github.com/najoshi/sickle> (2011).
59. Langmead, B. & Salzberg, S. L. Fast gapped-read alignment with Bowtie 2. *Nat. Methods* **9**, 357–359 (2012).
60. Li, H. et al. The Sequence Alignment/Map format and SAMtools. *Bioinformatics* **25**, 2078–2079 (2009).
61. Parnanen, K. et al. Maternal gut and breast milk microbiota affect infant gut antibiotic resistome and mobile genetic elements. *Nat. Commun.* **9**, 3891 (2018).
62. Venables, W. N. & Ripley, B. D. *Modern Applied Statistics with S-PLUS* (Springer Science & Business Media, 2013).
63. Miller, R. G. in *Simultaneous Statistical Inference* (ed. Miller, R. G.) 1–35 (Springer, 1981).
64. McMurdie, P. J. & Holmes, S. phyloseq: an R package for reproducible interactive analysis and graphics of microbiome census data. *PLoS ONE* **8**, e61217 (2013).

## Acknowledgements

We are grateful to A. Graveline for help with the animal protocol setup and A. Vernet and M. Sanchez-Ventura for assistance with animal experiments. We thank X. Tan, M. A. English, R. Gayet, D. Morales and J. Cubillos-Ruiz for helpful comments and discussions. We also thank K. Pärnänen for helpful discussion on metagenomic data processing and calculating antibiotic resistance gene abundances from metagenomic data. Additionally, we thank S. Blomquist for help with running analysis pipelines via the Commonwealth Computational Cloud for Data Driven Biology (C3DDB) cluster. This work was supported by funding from the Defense Threat Reduction Agency grant HDTRA1-14-1-0006 (to J.J.C.), Wyss Institute funding (to J.J.C.) and the Paul G. Allen Frontiers Group (to J.J.C.) and Wyss Institute validation project funding (to A.C.-R.). M.A.A. was supported by a National Science Foundation graduate research fellowship (award no. 1122374).

## Author contributions

A.C.-R. conceptualized the project, designed and performed experiments, analysed and interpreted data, acquired funding and wrote the manuscript. N.M.D. and J.A.-P. performed experiments; M.A.A. analysed data, performed experiments and wrote the manuscript; P.C. and J.A.-P. analysed data; and J.J.C. supervised the work, assisted with manuscript editing and acquired funding.

## Competing interests

J.J.C. is co-founder and SAB chair of Synlogic and EnBiotix. A.C.-R. and J.J.C. have filed a patent application for this work. The other authors declare no competing interests.

## Additional information

**Extended data** is available for this paper at <https://doi.org/10.1038/s41551-022-00871-9>.

**Supplementary information** The online version contains supplementary material available at <https://doi.org/10.1038/s41551-022-00871-9>.

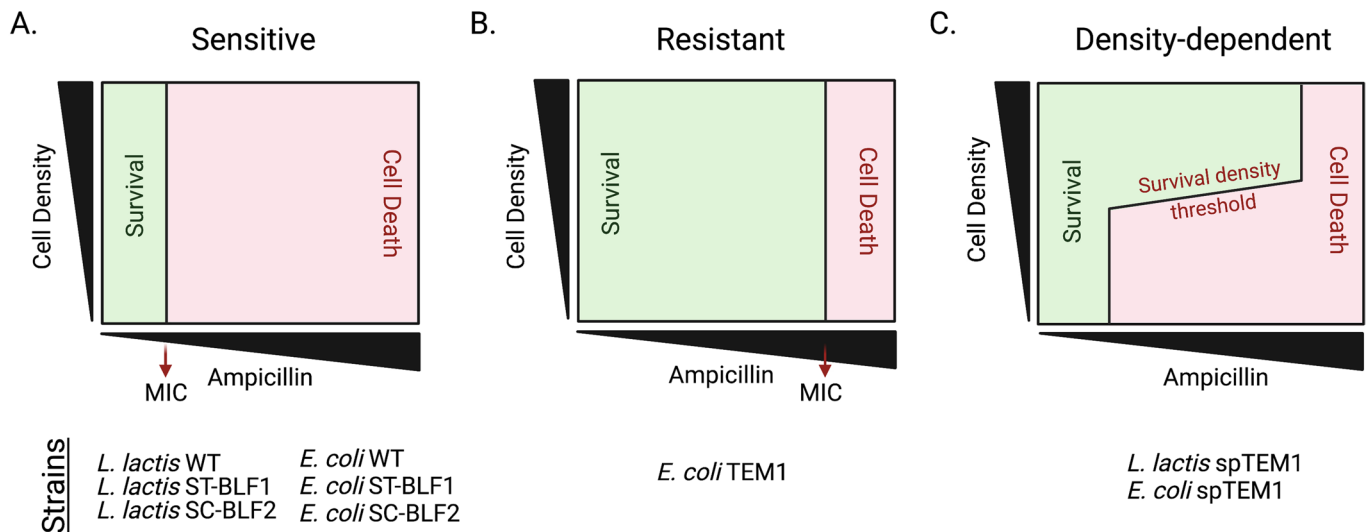
**Correspondence and requests for materials** should be addressed to James J. Collins.

**Peer review information** *Nature Biomedical Engineering* thanks Peter Turnbaugh and the other, anonymous, reviewer(s) for their contribution to the peer review of this work. Peer reviewer reports are available.

**Reprints and permissions information** is available at [www.nature.com/reprints](http://www.nature.com/reprints).

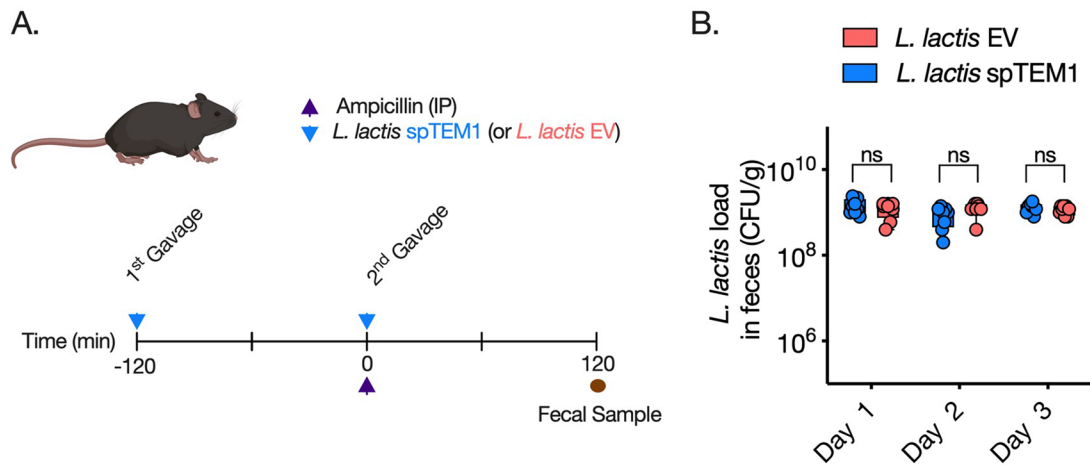
**Publisher's note** Springer Nature remains neutral with regard to jurisdictional claims in published maps and institutional affiliations.

© The Author(s), under exclusive licence to Springer Nature Limited 2022

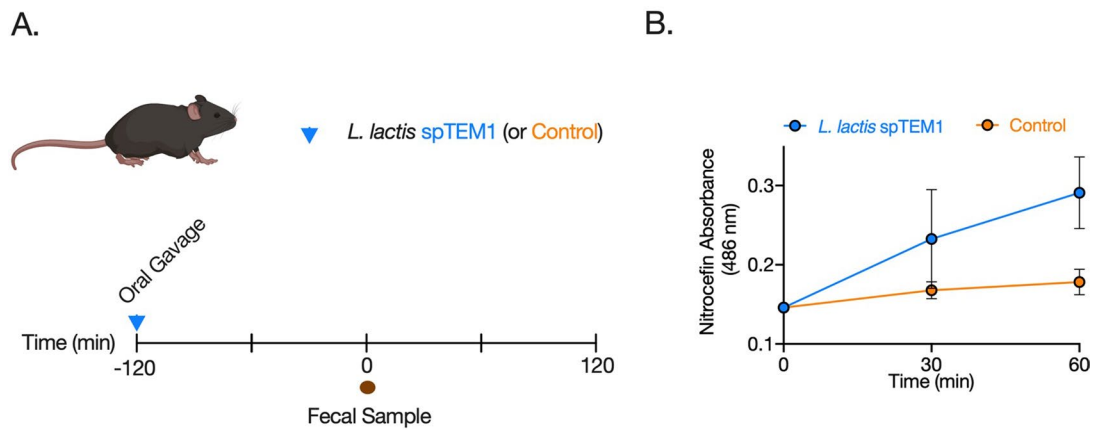


**Extended Data Fig. 1 | Schematic of the antibiotic survival landscape of the bacterial strains in this study.** **a.** In wildtype cells, the survival to the antibiotic is dictated by the minimum inhibitory concentration (MIC), which is the lowest concentration of an antibiotic that achieves inhibition of growth. In a population of antibiotic-sensitive cells, the landscape partition between survival and death is independent of cell density. **b.** Antimicrobial resistance factors (that is, native  $\beta$ -lactamase) decrease the susceptibility of the bacterial cell to the antibiotic, increasing the MIC. In a population of antibiotic-resistant cells, the partition between survival and death is also independent of cell density. **c.** Density-dependent survival effect in spTEM1-expressing strains. Secretion and extracellular assembly of the spTEM1  $\beta$ -lactamase preclude self-protection in producer cells and makes the partition of the antibiotic survival landscape a function of the cell density. Below the critical cell density threshold, the engineered cells are as susceptible to the antibiotic as wildtype cells. Above the cell density threshold, the engineered cells can survive the antibiotic to the same extent as their neighboring cells, offering population-wide protection.

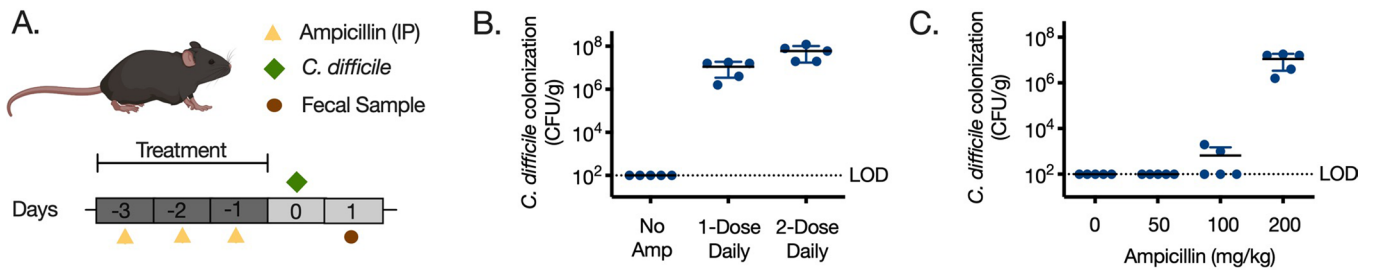




**Extended Data Fig. 2 | Determination of *L. lactis* load in the mouse intestine.** **a.** Treatment regimen. Mice were orally gavaged with two doses of  $10^{10}$  CFU of *L. lactis*. The first dose occurred 2 hours prior to the ampicillin injection and the second simultaneous with the 200 mg/kg ampicillin injection. Intestinal load was evaluated each day for *L. lactis* spTEM1 and the empty-vector control strain *L. lactis* EV. **b.** Enumeration of viable *L. lactis* cells in feces in each day of treatment demonstrates no difference in the fecal loads of *L. lactis* spTEM1 ( $n=8$ ) and *L. lactis* EV ( $n=8$ ). Box plots display minimum, 25th percentile, median, 75th percentile, and maximum of biological replicate measurements. Unpaired two-sided Wilcoxon test: Day 1,  $p=0.7944$ ; Day 2,  $p=0.0511$ ; Day 3,  $p=0.4093$ .

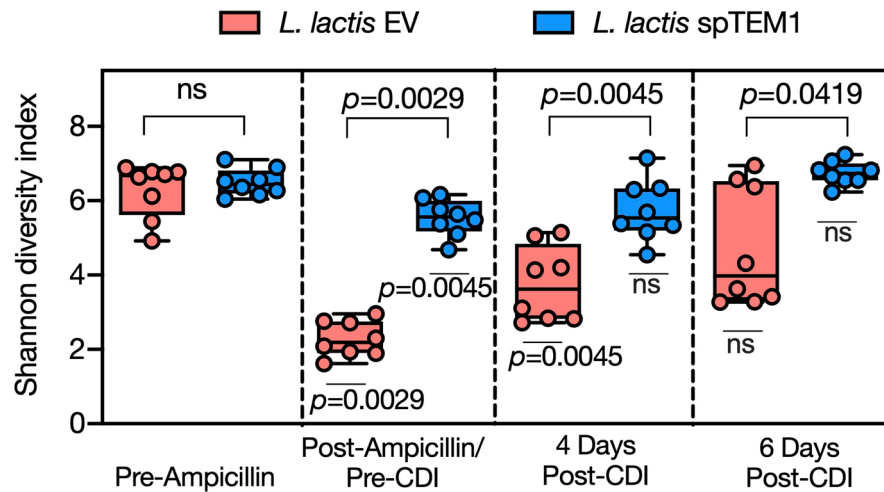


**Extended Data Fig. 3 | Detection of  $\beta$ -lactamase activity in fecal samples of ampicillin-naïve mice.** **a.** Fecal samples were collected 2 hours after a single dose of *L. lactis* spTEM1 or delivery vehicle control. **b.** Nitrocefin hydrolysis assay for the detection of  $\beta$ -lactamase activity. Means and standard deviations of biological replicates are shown.  $n=10$  mice in the *L. lactis* spTEM1 and control groups.

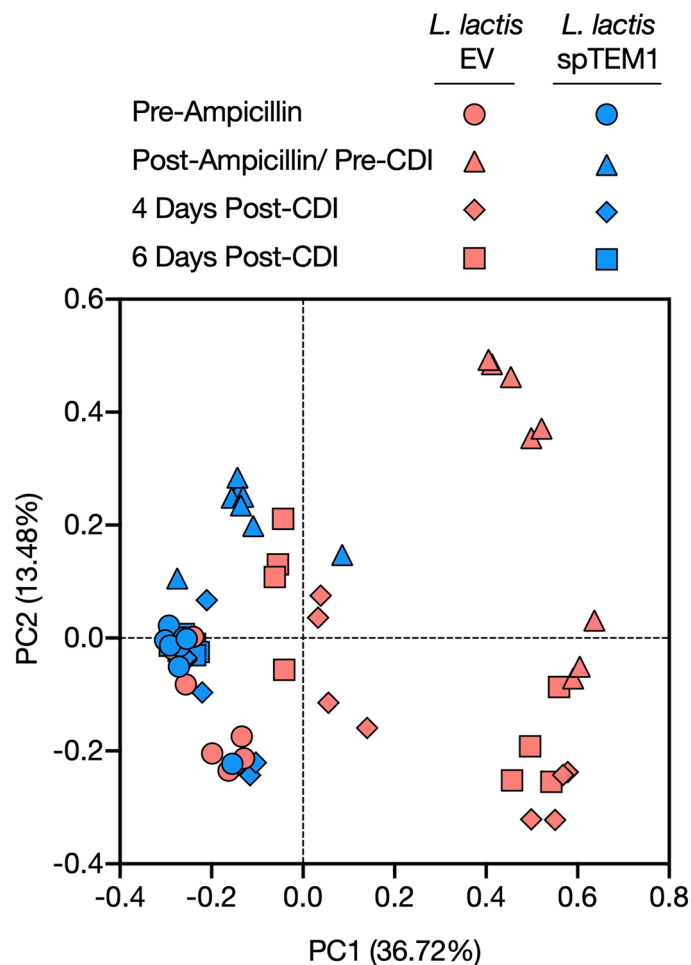


**Extended Data Fig. 4 | Mouse model for parenteral ampicillin-induced dysbiosis and the disruption of colonization resistance against *C. difficile*.** **a.** A 3-day intraperitoneal ampicillin administration regimen is evaluated for its effects in abolishing colonization resistance against  $5 \times 10^3$  spores of *C. difficile* at 24 hours after the last ampicillin dose. *C. difficile* density in feces is evaluated 24 hours after the infection. **b.** Evaluation of single- or double-dose (8 hours apart) administration regimens for intraperitoneal ampicillin injection indicates that a single dose of ampicillin for 3 days is enough to sensitize the mouse gut to robust *C. difficile* colonization.  $n = 5$  mice in each treatment group. Means and standard deviations of biological replicates are shown. **c.** Dose-dependency of single daily intraperitoneal ampicillin injections in the disruption of colonization resistance against *C. difficile*.  $n = 5$  mice in each treatment group. Means and standard deviations of biological replicates are shown.

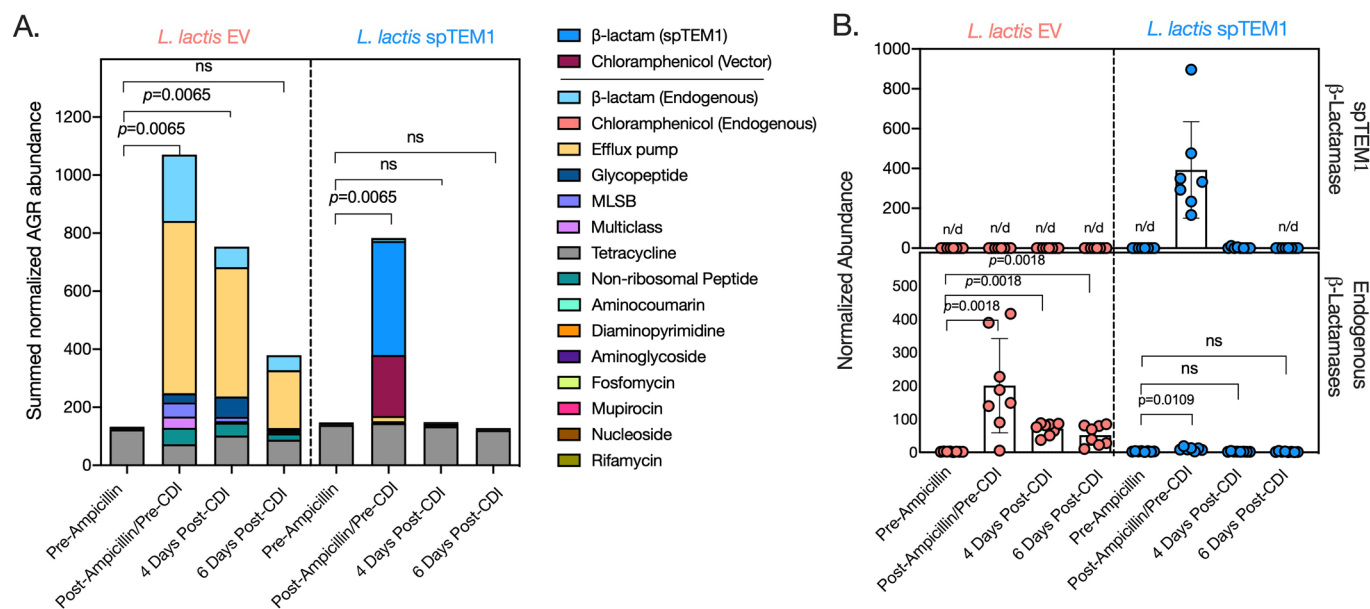
A.



B.



**Extended Data Fig. 5 | Diversity and composition of the gut microbiota during the experiment of preservation of colonization resistance against *C. difficile*.** **a.** Determination of the Shannon diversity index for gut microbial communities in mice pre- and post-treatment. The  $p$ -values correspond to FDR-corrected Wilcoxon tests between the groups that received *L. lactis* spTEM1 and *L. lactis* EV. Adjusted  $P$ -values below boxes correspond to FDR-corrected two-sided Wilcoxon tests comparing diversity values against baseline diversity at the pre-treatment timepoint. Box plots display minimum, 25th percentile, median, 75th percentile, and maximum of biological replicate measurements.  $n=8$  mice in each treatment group. **b.** Principal coordinates analysis of gut microbial communities in ampicillin-treated mice receiving *L. lactis* spTEM1 and *L. lactis* EV control reveals differences in the resulting composition of the community. Close clustering to pre-ampicillin conditions indicates smaller alterations in the community structure.  $n=8$  mice in each treatment group.



**Extended Data Fig. 6 | Metagenomic analysis of antimicrobial resistance genes (ARG) during the experiment of preservation of colonization resistance against *C. difficile*.** **a.** Analysis of the abundance of ARG reveals significant enrichment in ampicillin-treated mice receiving *L. lactis* EV but not in mice receiving *L. lactis* spTEM1. Stacked bar data are presented as reads mapping the different CARD database categories and normalized to the size of the read pool in each sample. Vector-derived ARG in the  $\beta$ -lactam and chloramphenicol classes are presented as a different category to differentiate them from endogenous ARG. Adjusted  $p$ -values were calculated with a negative binomial generalized linear model with Tukey's post hoc test between spTEM1-treated and EV-treated groups. **b.** Abundance of endogenous and *L. lactis* spTEM1-derived  $\beta$ -lactamases in the mouse. Elimination of the ampicillin selective pressure by the spTEM1  $\beta$ -lactamases reduces the enrichment of endogenous  $\beta$ -lactamases in the mouse gut. Rapid elimination from the system of the spTEM1 gene fragments compared to endogenous  $\beta$ -lactamase genes suggests lack of competitive advantage in the spTEM1 strain.  $n = 8$  mice in each *L. lactis* spTEM1 and *L. lactis* EV groups.  $p$ -value significance corresponds to FDR-corrected two-sided Wilcoxon tests comparing ARG abundance values against baseline values at the pre-treatment timepoint. Means and standard deviations of biological replicates are shown.



## Reporting Summary

Nature Research wishes to improve the reproducibility of the work that we publish. This form provides structure for consistency and transparency in reporting. For further information on Nature Research policies, see our [Editorial Policies](#) and the [Editorial Policy Checklist](#).

### Statistics

For all statistical analyses, confirm that the following items are present in the figure legend, table legend, main text, or Methods section.

n/a Confirmed

- |                                     |                                     |  |
|-------------------------------------|-------------------------------------|--|
| <input type="checkbox"/>            | <input checked="" type="checkbox"/> | The exact sample size ( $n$ ) for each experimental group/condition, given as a discrete number and unit of measurement  |
| <input type="checkbox"/>            | <input checked="" type="checkbox"/> | A statement on whether measurements were taken from distinct samples or whether the same sample was measured repeatedly  |
| <input type="checkbox"/>            | <input checked="" type="checkbox"/> | The statistical test(s) used AND whether they are one- or two-sided<br><i>Only common tests should be described solely by name; describe more complex techniques in the Methods section.</i>   |
| <input checked="" type="checkbox"/> | <input type="checkbox"/>            | A description of all covariates tested   |
| <input type="checkbox"/>            | <input checked="" type="checkbox"/> | A description of any assumptions or corrections, such as tests of normality and adjustment for multiple comparisons  |
| <input type="checkbox"/>            | <input checked="" type="checkbox"/> | A full description of the statistical parameters including central tendency (e.g. means) or other basic estimates (e.g. regression coefficient) AND variation (e.g. standard deviation) or associated estimates of uncertainty (e.g. confidence intervals) |
| <input type="checkbox"/>            | <input checked="" type="checkbox"/> | For null hypothesis testing, the test statistic (e.g. $F$ , $t$ , $r$ ) with confidence intervals, effect sizes, degrees of freedom and $P$ value noted<br><i>Give <math>P</math> values as exact values whenever suitable.</i>                            |
| <input checked="" type="checkbox"/> | <input type="checkbox"/>            | For Bayesian analysis, information on the choice of priors and Markov chain Monte Carlo settings   |
| <input checked="" type="checkbox"/> | <input type="checkbox"/>            | For hierarchical and complex designs, identification of the appropriate level for tests and full reporting of outcomes   |
| <input checked="" type="checkbox"/> | <input type="checkbox"/>            | Estimates of effect sizes (e.g. Cohen's $d$ , Pearson's $r$ ), indicating how they were calculated   |

*Our web collection on [statistics for biologists](#) contains articles on many of the points above.*

### Software and code

Policy information about [availability of computer code](#)

**Data collection** SoftMax Pro 7.1 GxP software was used for absorbance-data acquisition. TraceFinder (version 3.3, Thermo Fisher Scientific; Waltham, MA) was used for MS peak data acquisition. GeneTools analysis software was used for image acquisition.

**Data analysis** We used PRISM v8.4.1 (GraphPad; San Diego, CA) for some statistical analysis and data plotting, and QIIME 2 (Core 2020.2 distribution) for microbial-diversity analysis (detailed in Methods). Other software used for data processing and for the statistical analyses is detailed in Methods.

For manuscripts utilizing custom algorithms or software that are central to the research but not yet described in published literature, software must be made available to editors and reviewers. We strongly encourage code deposition in a community repository (e.g. GitHub). See the Nature Research [guidelines for submitting code & software](#) for further information.

### Data

Policy information about [availability of data](#)

All manuscripts must include a [data availability statement](#). This statement should provide the following information, where applicable:

- Accession codes, unique identifiers, or web links for publicly available datasets
- A list of figures that have associated raw data
- A description of any restrictions on data availability

The main data supporting the results in this study are available within the paper and its Supplementary Information. Source data for the figures are provided with this paper. All DNA sequence data generated in this study are available from the Sequence Read Archive (SRA) with accession number PRJNA803721.

## Field-specific reporting

Please select the one below that is the best fit for your research. If you are not sure, read the appropriate sections before making your selection.

Life sciences       Behavioural & social sciences       Ecological, evolutionary & environmental sciences

For a reference copy of the document with all sections, see [nature.com/documents/nr-reporting-summary-flat.pdf](https://www.nature.com/documents/nr-reporting-summary-flat.pdf)

## Life sciences study design

All studies must disclose on these points even when the disclosure is negative.

Sample size	No statistical methods were used to predetermine sample size. Pilot studies were performed with 4–5 mice per group, and were used to inform subsequent experiments with a sample size of 5–10 mice per group.
Data exclusions	The exclusion of data points owing to accidental animal loss or to technical failures of data acquisition is detailed in Methods.
Replication	Replicate experiments were performed and noted in figure legends and in Methods. In vitro experiments were performed at least with three independent biological samples, and the variability between biological replicates was low. For the mouse studies, 4–8 animals per group were used, and the experiments were performed at least twice, to ensure reproducibility.
Randomization	After the 5-day acclimation period on arrival to the mouse facility, the mice were randomly assigned to experimental or control groups in defined cages. Within-cage randomization was not possible owing to coprophagy, which could create confounding experimental outcomes.
Blinding	The investigators carrying out the mouse manipulations were blinded to the identity of the contents in the syringes used for injections, and gavages as samples were labelled by code only. No additional blinding was performed.

## Reporting for specific materials, systems and methods

We require information from authors about some types of materials, experimental systems and methods used in many studies. Here, indicate whether each material, system or method listed is relevant to your study. If you are not sure if a list item applies to your research, read the appropriate section before selecting a response.

### Materials & experimental systems

n/a	Involved in the study
<input checked="" type="checkbox"/>	<input type="checkbox"/> Antibodies
<input checked="" type="checkbox"/>	<input type="checkbox"/> Eukaryotic cell lines
<input checked="" type="checkbox"/>	<input type="checkbox"/> Palaeontology and archaeology
<input type="checkbox"/>	<input checked="" type="checkbox"/> Animals and other organisms
<input checked="" type="checkbox"/>	<input type="checkbox"/> Human research participants
<input checked="" type="checkbox"/>	<input type="checkbox"/> Clinical data
<input checked="" type="checkbox"/>	<input type="checkbox"/> Dual use research of concern

### Methods

n/a	Involved in the study
<input checked="" type="checkbox"/>	<input type="checkbox"/> ChIP-seq
<input checked="" type="checkbox"/>	<input type="checkbox"/> Flow cytometry
<input checked="" type="checkbox"/>	<input type="checkbox"/> MRI-based neuroimaging

## Animals and other organisms

Policy information about [studies involving animals](#); [ARRIVE guidelines](#) recommended for reporting animal research

Laboratory animals	6-to-8-week-old female C57BL/6 mice (Charles River Laboratories) were used for the experiments.
Wild animals	The study did not involve wild animals.
Field-collected samples	The study did not involve samples collected from the field.
Ethics oversight	All mice were treated in accordance with protocol IS00000852-3, approved by the Harvard Medical School Institutional Animal Care and Use Committee and by the Committee on Microbiological Safety.

Note that full information on the approval of the study protocol must also be provided in the manuscript.